Received February 4, 2020, accepted March 15, 2020, date of publication March 17, 2020, date of current version March 26, 2020.

Digital Object Identifier 10.1109/ACCESS.2020.2981555

Multi-Source Feature Fusion and Entropy Feature Lightweight Neural Network for Constrained Multi-State Heterogeneous Iris Recognition

LIU SHUAI[1,2], LIU YUANNING[1,2], ZHU XIAODONG[1,2], HUO GUANG[3], CUI JINGWEI[2,4], ZHANG QIXIAN[2,4], WU ZUKANG[1,2], LI XINLONG[2,4], AND WANG CHAOQUN[2,4]

[1]College of Computer Science and Technology, Jilin University, Changchun 130012, China
[2]Key Laboratory of Symbolic Computation and Knowledge Engineering of Ministry of Education, Jilin University, Changchun 130012, China
[3]College of Computer Science, Northeast Electric Power University, Jilin 132012, China
[4]College of Software, Jilin University, Changchun 130012, China

Corresponding author: Zhu Xiaodong (zhuxd@jlu.edu.cn)

This work was supported in part by the National Natural Science Foundation of China (NSFC) under Grant 61471181, in part by the Natural Science Foundation of Jilin Province under Grant 20140101194JC and Grant 20150101056JC, in part by the Jilin Province Industrial Innovation Special Fund Project under Grant 2019C053-2, in part by the Science and Technology Project of the Jilin Provincial Education Department under Grant JJKH20180448KJ, and in part by the Jilin Provincial Key Laboratory of Biometrics New Technology.

ABSTRACT Current iris recognition technology faces practical difficulties. For example, due to the unsteady morphology of a heterogeneous iris generated by a variety of different devices and environments, the traditional processing methods of statistical learning or cognitive learning for a single iris source are not effective. The existing iris data set size and situational classification constraints make it difficult to meet the requirements of learning methods under a single deep learning framework. Therefore, this paper proposes a method of heterogeneous iris recognition based on an entropy feature lightweight neural network under multi-source feature fusion. The method is divided into an image-processing module and a recognition module. The image-processing module converts the iris image into a recognition label via a convolutional neural network. The recognition module is based on statistical learning ideas and design of a multi-source feature fusion mechanism. The information entropy of the iris feature label is used to set the iris entropy feature category label and design the recognition function according to the category label to obtain the recognition result. As the requirement for the number and quality of irises changes, the category labels in the recognition function are dynamically adjusted using a feedback learning mechanism. This paper uses iris data collected from three different devices in the JLU iris library. The experimental results prove that for multi-category classification of lightweight constrained multi-state irises, the abovementioned problems are ameliorated to a certain extent by this method.

INDEX TERMS Heterogeneous iris recognition, constrained multi-state, multi-source feature fusion, entropy feature, lightweight neural network, feedback learning mechanism.

I. INTRODUCTION

Iris recognition is currently one of the higher security technologies recognized in the field [1], and its core is the expression and matching of iris features.

In iris collection, the main settings are the collection status (collection posture, collection distance) and the external environment (illumination), which can be divided into four categories:

1. Unconstrained state in the same environment: Iris acquisition is performed based on no restriction of the acquisition posture of the acquisition target person, and the external environment is not changed for iris acquisition;
2. Constrained state in the same environment: Iris acquisition is performed based on restriction of the acquisition posture of the acquisition target person, and the external environment is not changed for iris acquisition;
3. Constrained state of environmental change: Iris acquisition is performed based on restriction of the

The associate editor coordinating the review of this manuscript and approving it for publication was Shuihua Wang.

acquisition posture of the acquisition target person, and the external environment is changed for iris acquisition;
4. Unconstrained state of environmental change: Iris acquisition is performed based on no restriction of the acquisition posture of the acquisition target person, and the external environment is changed for iris acquisition.

According to the result, the process of recognition can be divided into two types: template matching and non-template matching. Template matching identifies the test iris with a single stored template iris and obtains the final conclusion. This process can be divided into one-to-one certification (to determine whether the test iris and the template iris belong to the same person) and one-to-many recognition (the iris of the test person is matched with multiple template irises, and the identity of the test person must be accurately identified). Non-template matching usually forms the features of the iris into a cognitive concept and integrates them into neural network architectures such as deep learning in the form of parameters [2] to achieve uncoded matching recognition.

In the current application scenarios, multi-category recognition is the most research-oriented direction. In the multi-category recognition scenario, the case of lightweight absolute recognition exists; i.e., when the number of trained irises is not large, the identity of a person must be recognized 100% correctly. In such cases, it is necessary to ensure a high degree of discrimination of iris features and a high accuracy of the iris recognition method. Given the research on iris feature expression and recognition for this purpose, the following aspects still require further breakthroughs.

1. Iris multi-state and single-source feature expression: Most training and learning recognition models in the current iris multi-category recognition algorithms are based on publicly known iris training sets (such as CASIA iris set [3], Ubiris [4]) or manually set iris labels. However, in the actual shooting process, multi-state heterogeneity is expected to occur between the template image and the collected image. There are many reasons for the multi-state, and they are divided into three main aspects:

1. The acquisition devices are different (e.g., NIR device [5] and ordinary optical camera [6]; iris sample pictures taken by different cameras are shown in FIGURE 1).
2. The collection environment is different because the iris status is unstable under different environments (illumination, etc.), which affects the relative relationship between the iris textures.
3. The acquisition status of the iris is different. Because the acquisition status of the target person varies at different times, disturbances such as defocusing and deflection occur.

Because the algorithm applied in the process of iris processing and recognition takes on a black box state, it is impossible to predict the outcome, which makes it difficult to design a unified process for the variable and unsteady iris using fixed parameters and to subsequently form selected effects for iris quality, localization and feature expression;

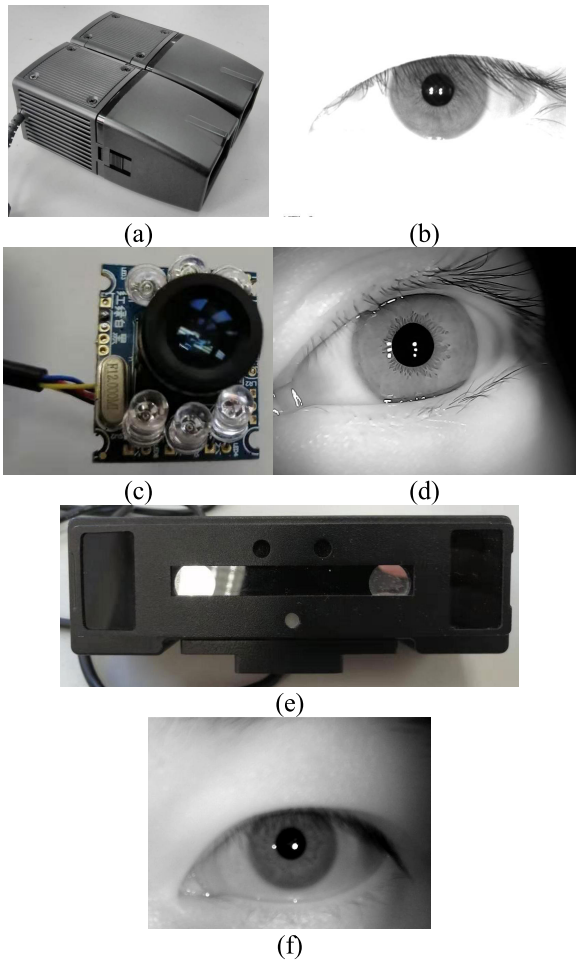

FIGURE 1. Eye collection equipment(a) NIR acquisition equipment, (b) NIR acquisition equipment for ideal images, (c) Ordinary optical acquisition equipment, (d) Ordinary optical acquisition equipment for ideal images, (e) Ordinary optical acquisition equipment for upgrading sensors, (f) Ordinary optical acquisition equipment with upgraded sensors corresponds to ideal images.

this difficulty leads to the unsteady nature of iris features. An example of a multi-state iris (taking the same device and the same person as an example) is shown in FIGURE 2.

It can be observed from Figure 2 that even the same device and the same person cannot guarantee the final appearance of the iris feature, which can affect the expression of the iris feature. Therefore, research on the impact of a multi-state iris on setting of iris labels requires further examination.

2. Concept label setting and universal recognition of heterogeneous iris datasets: Currently, two main forms of iris concept label setting exist. Statistical learning methods [7]: Through analysis of the notably large amount of data in the same type of situation, a reasonable solution is obtained that meets the vast majority of requirements. Cognitive learning methods [8]: By imitating the process of human learning, labels are set on things to form the concept of things. The statistical learning method is currently the most commonly used method, and it applies a good combination of deep learning

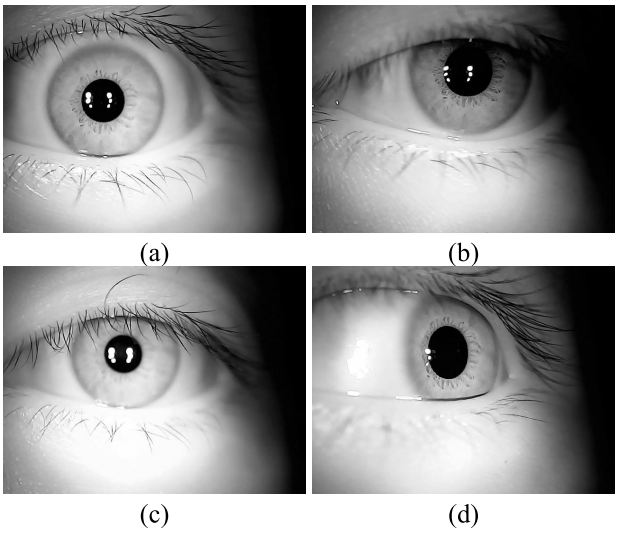

FIGURE 2. An example of a multi-state iris, (a) normal iris, (b) iris with dark condition, (c) iris with defocused condition, (d) iris with deflected condition.

and other aspects. However, this type of method has high requirements for data preparation. In addition to requiring large amounts of data, this type of method also requires a clear division of the type of irises, and the limitations of the existing iris dataset size and situation classification make it difficult to meet a single depth. The amount of data required for the learning method under the learning framework also makes it difficult to support the establishment of a self-improvement process from forward recognition to the reverse. In addition, the accumulation of iris multi-case data cannot be completed in a short time, which greatly limits the role of statistical learning. Although cognitive learning can reduce the need for data volume, the relationship between the iris labels and unknown environments needs further research. Because the hardware configuration between different collectors and the environment in which they are collected is expected to vary at different times, and the algorithm itself has prerequisites for use, and this situation makes the recognition effect of the same algorithm differ substantially in different situations, thus greatly increasing the design complexity of iris recognition algorithms.

These problems make the iris more accurate in multi-class recognition. In efforts to solve these problems, certain progress has been reported in current research on the expression and recognition of iris features.

In the current research, the importance of the entire iris recognition process has begun to emerge because the effect of iris quality evaluation and positioning is manifested through the results of feature expression and recognition, and conversely, the recognition results also show that iris quality and iris positioning determine whether the effect is feasible. As a result, additional studies have begun to focus attention on the overall relationship and design for the framework, such as iris-specific Mask R-CNN [9], to modify the existing framework, integrate the positioning into the iris recognition process, and publicly test the iris set to prove the feasibility of the framework. In research on the unsteady-state iris, the unsteady-state features are transformed into steady-state features through image processing and other methods [10], and the iris features are expressed through multiple recognition methods and weighted fusion [11] or the final result is obtained based on a credibility decision [12]. For setting of iris concept labels, research on biomimetic cognition [13] is an important direction, i.e., determination of how to first summarize a feasible recognition model in the case of a small number of initial training samples, and with increases in the number of recognitions and available training samples, how to further effectively judge whether the current structure cannot meet the existing situation and requires users to retrain [14]. A current proposal is to set the iris label for the statistical cognitive learning method of unclassified mixed data [15] and apply the MiCoRe-Net neural network architecture [16] for eye concept reconstruction. In addition, for label correction of the existing neural network architecture, an error correction code-based label optimization method [17] and a feedback mechanism-based label correction method [18] have been proposed. In the study of iris generality, heterogeneous iris recognition is the main direction [19]. First, by changing the internal structure of the algorithm, the device independence of the iris image is improved [20]. Second, correction of images (blurring, displacement, etc.) using algorithms [21] improves the feasibility of multi-type iris recognition and further improves the environmental independence.

Previous studies have achieved good results in various experiments, but selected problems remain, and thus, the need exists to improve the accuracy of iris multi-category recognition.

1. The existing structural framework is designed to process a certain type of data, and the design purpose of the framework is not necessarily aimed at iris recognition. When the existing framework is used in iris recognition, inputting the iris data directly into the frame might not achieve a good recognition effect. The unsteady-state iris in an uncertain state is prone to the situation in which the existing framework does not match the input iris data. When the iris data set is limited in size, classification of the situation is limited, and altering the existing framework might reduce the accuracy of recognition, thus greatly limiting the types of existing frameworks that can be used. The question of how to design the framework to better adapt to the iris data must be addressed.
2. In study of feature expression and universal recognition, most methods normalize the data of different devices and different environments using algorithms such that the images can be identified under the same standard. However, not all processes are suitable for all images; this lack of suitability can cause unnecessary calculations and exclude certain images that can

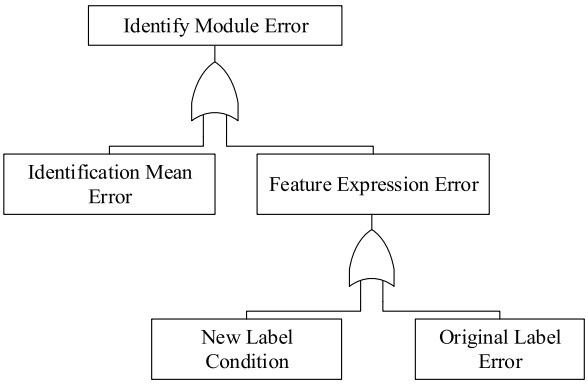

FIGURE 3. Fault tree for common iris recognition error cases (only in terms of feature expression and recognition).

be identified but are not considered to be available irises because they do not meet the standard iris, possibly resulting in a lack of training of the unsteady iris model. Current research lacks a universal process mechanism for the heterogeneous iris generated in a variety of different devices and environments. Because a single algorithm is prone to omission in unsteady-state features, many algorithms use multi-source feature expressions, an approach that requires in-depth understanding of the relationship between different types of features to avoid repeated calculation of iris features with large correlations and to improve the remoteness and discrimination of features.

3. With the limited size of the iris data set and the limitation of situation classification, it is necessary to judge the situation of recognition errors and establish a reverse correction mechanism for the recognition framework process. This mechanism not only avoids mechanical judgment by relying on a large amount of data to generate fixed indicators in statistical learning but also avoids the situation of cognitive loss caused by the inability to form new concepts when unknown situations occur in cognitive learning.

Therefore, in actual iris recognition, the recognition accuracy of the multi-state iris in a multi-category scenario will still be low. In terms of feature expression and recognition, selected common causes are represented in the form of a fault tree, as shown in FIGURE 3.

According to the current problems of iris multi-classification research, we analyze the situation that might cause errors, as shown in FIGURE 3. This paper proposes solutions for the following problems:

1. In facing the unsteady situation of heterogeneous iris morphology produced by a variety of different devices and environments, the traditional processing method of a single source iris based on statistical learning or cognitive learning is not effective;
2. Traditional iris recognition divides the entire process machinery into several statistically guided steps, which cannot solve the problem of correlation between various links;
3. The existing iris dataset size and situation classification constraints make it difficult to meet the requirements of learning methods in a single deep learning framework.

Therefore, this paper takes lightweight one-to-many recognition of a multi-state iris with the same environment constraints as the research object, proposes a multi-category recognition method based on a multi-source fusion entropy feature neural network, and makes the overall process follow With a change in the number of irises, the category labels in the recognition function are dynamically adjusted.

The prerequisites for this method are listed as follows:

1. The iris acquisition status and acquisition environment change, and this change cannot be predicted, which causes certain defocusing, deflection, shadowing and other problems. The dimensions of the captured images are 640×480;
2. The number of iris categories is lightweight (all iris libraries contain dozens of categories, and each category contains only a few thousand pictures);
3. To ensure the accuracy of lightweight recognition, testers are allowed to collect multiple times, and thus, it is allowable to appropriately increase the false rejection rate;
4. The number of training irises can reach several thousand, but the types of training irises (degree of defocus, illumination, strabismus effect, etc.) are not classified; they are directly mixed, belonging to mixed data;
5. The subject tester is a living human.

Based on the convolutional neural network structure, this paper divides the recognition process into an image-processing module and recognition module. In the image-processing module, the image of the iris recognition area is processed by a smoothing algorithm and a texture highlighting algorithm. Three different iris images are formed as multi-source features. Each iris image passes through 12 layers of an image-processing network consisting of convolutional layer, pooling layer, ReLU layer, and expansion layer. Finally, each iris image forms 15 expanded parameters and a total of 45 expanded parameters in the expansion layer. In the recognition module, the expanded parameters of the 3 images are fused by average fusion through the feature fusion layer to form 15 recognition parameters. The recognition function is designed based on the sigmoid function [22], and the statistical information is used to calculate the recognition parameter information entropy. According to the information entropy, the recognition function parameters are designed as the category labels. In the fully connected layer, multi-category recognition is finally performed through the recognition function, and finally, the final result is output through the output layer. We design a feedback learning mechanism for the category labels, check the existing category labels, and correct them based on changes in the number of irises.

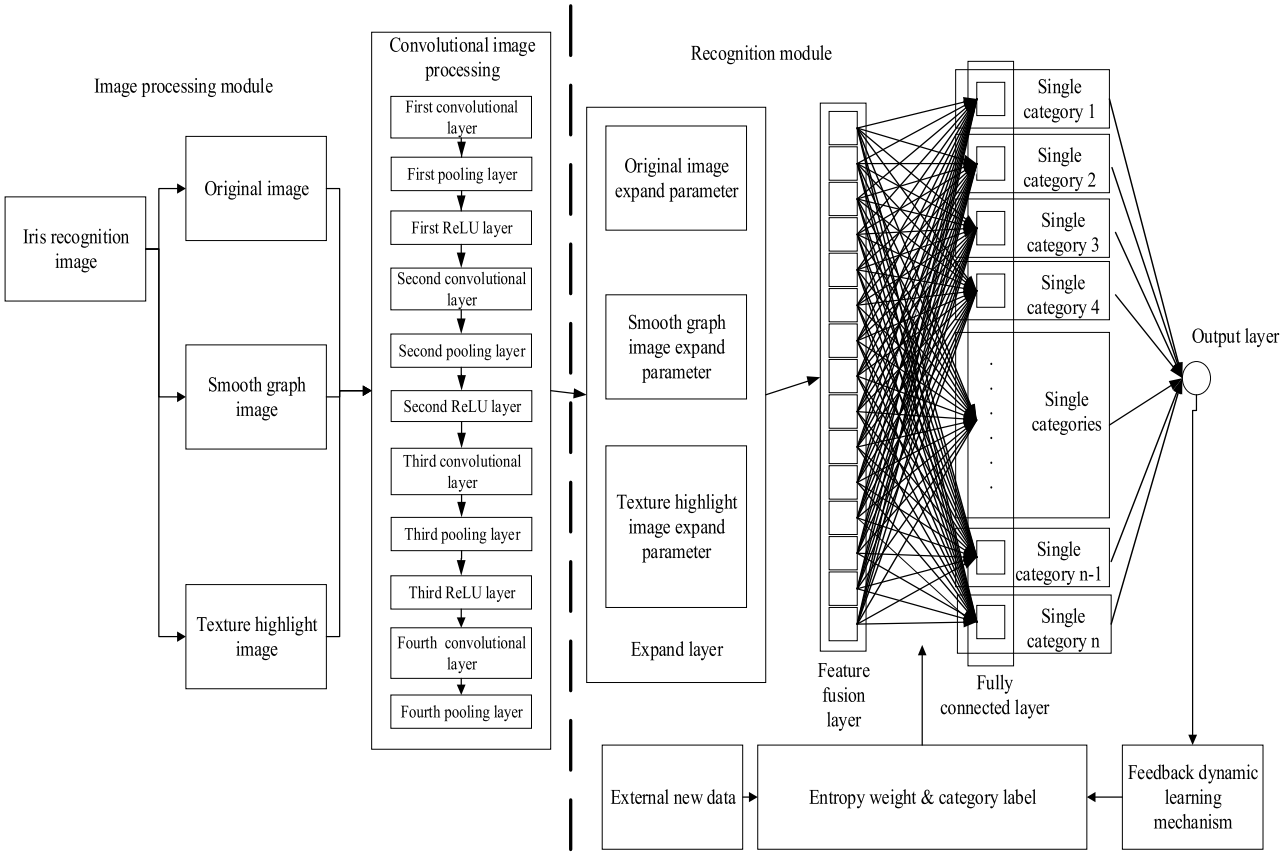

FIGURE 4. The overall working process of the method in this paper.

Compared with the current research, the innovation and research significance of this method in terms of improving the accuracy of multi-category recognition are described as follows:

1. **The problem of the heterogeneous constraint multi-state iris:** In feature expression, a multi-source feature fusion mechanism is designed, feature fusion is performed from a multi-source perspective, and discrimination between different types of features is increased. The information entropy is used to design the recognition function category label parameters, realize the statistical recognition of the unsteady-state iris in the mixed data set, expand the range of recognizable iris, and improve the accuracy of constrained multi-state heterogeneous iris recognition.
2. **Relevance of feature expression and recognition:** In this paper, the non-template matching mode is used as the basis for design of the recognition model. It is not confined to a specific algorithm for research but primarily focuses on research of the protocol mechanism. Feature expression and recognition are interconnected, and the correlation between the two steps is fully considered. Based on the instability of the multi-state iris, and with the aim of making the scheme universal, lightweight multi-category heterogeneous recognition can be realized, i.e., iris images collected under different environments in different devices can be identified by this scheme.
3. **Limitations on iris dataset size and situation classification:** Based on improvement of the positive recognition process, this paper designs a feedback learning mechanism in the revision of the reverse overall process. Via professional analysis by human operators and data feedback from the computer system, the error recognition situation and new possible external conditions are added. In this way, the process of performing a response and adjusting or correcting the entropy characteristics of the category labels enables the entire recognition process to achieve dynamic adjustment, thus improving the forward recognition and reverse correction of deep learning frameworks under the data set constraints.

The overall working process of the method proposed in this paper is shown in FIGURE 4.

The remainder of this paper is organized as follows. In Section 2, the workflow of the proposed method is introduced from three aspects: iris processing, multi-source and multi-feature fusion mechanism, and heterogeneous

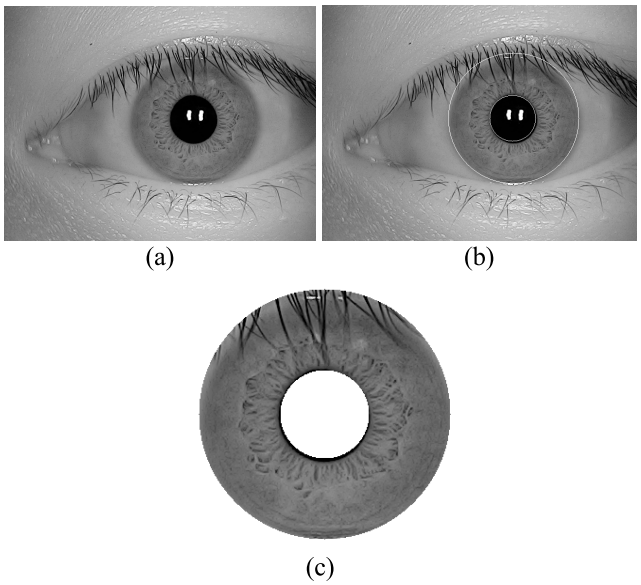

FIGURE 5. The image of each stage of positioning (a) quality qualified image, (b) positioning image, (c)segmentation image.

recognition. Moreover, the related functions are presented, and their meanings are explained. In Section 3, the rationality and reasons for the setting of each component of the method are explained in the form of data with explanation of the structural meaning. The performance of this method in multi-classification is demonstrated in experiments, and the advantages are illustrated by comparison with other methods in comprehensive experiments. Finally, conclusions are drawn in Section 4.

II. HETEROGENEOUS IRIS RECOGNITION

Under the premise that the amount of data is small and that various states cannot be accurately classified, it can only be identified based on mixed data. Therefore, a lightweight neural network structure that can identify this situation must be designed to meet the requirements of feature label setting and heterogeneous multi-category recognition. In this paper, an iris recognition structure based on the convolutional neural network [23] is used.

A. IRIS PROCESSING

Iris images must be processed prior to feature extraction. Iris images that cannot complete the recognition process are eliminated by quality evaluation [24]. Subsequently, the iris region is segmented [25] and mapped to a fixed dimension by the Daugman rubber band method[26]. In this paper, the normalized iris image has dimensions of 360×64, and the 180×32 dimensional area is taken from the upper left corner as the recognition area. In the actual iris acquisition process, under the external environmental influences such as illumination, defocusing and deflection and change of the collector state, many states of iris presentation might occur. To ensure the efficiency of shooting and recognition, the qualified standard

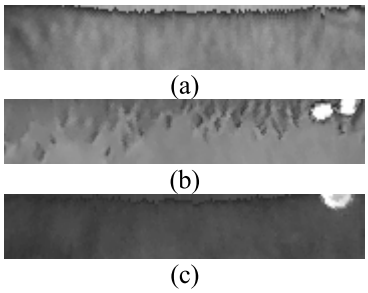

FIGURE 6. Examples of iris recognition areas of different iris libraries, (a) iris recognition area of Figure 1(b), (b) iris recognition area of Figure 1(d), (c) iris recognition area of Figure 1(f).

of the iris quality evaluation method for continuous frames is low, and only extreme conditions with poor iris quality are removed. The image of each stage of positioning is shown in FIGURE 5. Examples of iris recognition areas of different iris libraries are shown in FIGURE 6.

B. MULTI-SOURCE AND MULTI-FEATURE FUSION MECHANISM AND HETEROGENEOUS RECOGNITION

A multi-source multi-feature fusion mechanism for iris feature extraction is established. Under this mechanism, the image of the iris recognition area is processed by the smoothing algorithm and the texture highlighting algorithm. Each iris image passes through 12 layers of an image-processing network consisting of a convolutional layer, pooling layer, ReLU layer, and expansion layer. Finally, each iris image forms 15 expanded parameters and a total of 45 expanded parameters in the expansion layer. In the recognition module, the expanded parameters of the 3 images are fused by average fusion through the feature fusion layer to form 15 recognition parameters.

1) MULTI-SOURCE FEATURES AND IMAGE PROCESSING

The traditional single-angle statistical learning method encounters difficulty in collecting the multi-state iris. Therefore, a multi-source method is used to express the features from multiple angles. Smooth filtering and texture highlight filtering are applied. It is to better find a stable region that can reflect the texture change relationship inside the iris and to suppress the influence of illumination and defocusing on the feature expression as much as possible.

This paper uses Gaussian filtering (smoothed) and the equalization histogram (highlighted) as examples to explain the image-processing network. An example of the filtered image in Figure 6 is shown in FIGURE 7.

Each image is processed through the same image-processing module. The specific steps of the image-processing module are listed as follows:

First step: An iris image is input into the first convolutional layer. A gradient Laplacian convolution kernel is used. After image convolution, the image is converted into 2×2 maximum pooling in the first pooling layer, a 90×16

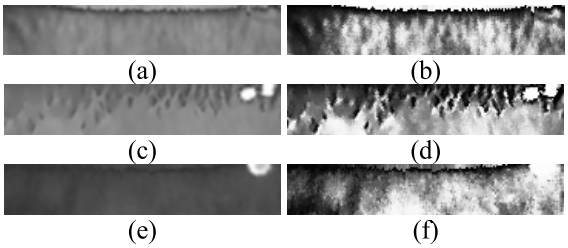

FIGURE 7. An example of the filtered image (a) Gaussian filtering of Figure 6(a), (b) Equalization histogram of Figure 6(a), (c) Gaussian filtering of Figure 6(b), (d) Equalization histogram of Figure 6(b), (e) Gaussian filtering of Figure 6(c), (f) Equalization histogram of Figure 6(c).

1	1	1
1	−8	1
1	1	1

FIGURE 8. Gradient Laplacian convolutional kernel of the first convolutional kernel.

dimensional image, thus thinning the pooled image through the Softplus function in the first ReLU layer.

The Softplus function is shown in Equation 1:

$$Softplus(x) = \log(1 + e^x) \tag{1}$$

where x represents the gray value of each point of the first pooling image, and $Softplus(x)$ is the resulting value of each point of the first ReLU image.

The convolutional kernel of the first convolutional layer is shown in FIGURE 8.

Finally, the result in the first ReLU layer is one processed image.

Second step: The second convolutional layer uses three convolution kernels, namely, the gradient Laplacian convolution kernel, horizontal Sobel convolution kernel, and vertical Sobel convolution kernel. The gradient Laplacian convolution kernel is the same as the first convolution layer. After a ReLU image is convolved, three convolutional images are formed. The image is converted into a 45 × 8-dimensional image by 2 × 2 maximum pooling in the second pooling layer and the Softplus function in the second ReLU layer The second ReLU layer uses the same Softplus function as the first ReLU layer to perform thinning operations on the pooled images in the second pooling layer.

The convolutional kernels of the second convolutional layer are shown in FIGURE 9.

The result in the second ReLU layer is three processed images.

Third step: The third convolutional layer uses five convolution kernels, namely, the gradient Laplacian convolution kernel, horizontal Sobel convolution kernel, vertical Sobel convolution kernel, horizontal gradient convolution kernel, and vertical gradient convolution kernel. The gradient

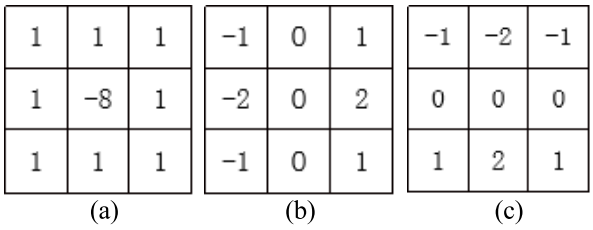

FIGURE 9. Convolutional kernels of the second convolutional layer: (a) gradient Laplacian convolutional kernel, (b) horizontal Sobel convolutional kernel, and (c) vertical Sobel convolutional kernel.

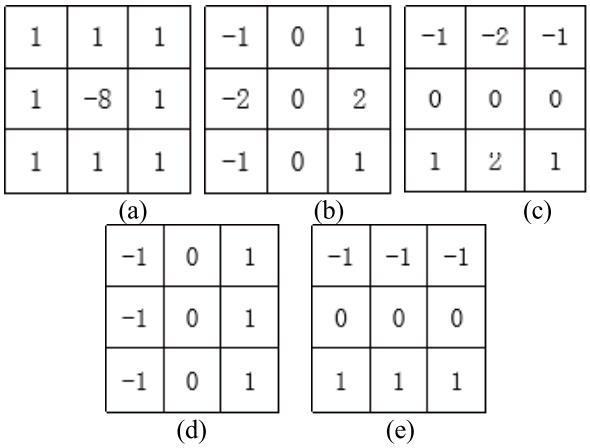

FIGURE 10. Convolutional kernels of the third convolutional layer (a) gradient Laplacian convolutional kernel, (b) horizontal Sobel convolutional kernel, (c) vertical Sobel convolutional kernel, (d) horizontal gradient convolutional kernel, (e) vertical gradient convolutional kernel.

Laplacian convolution kernel is the same as the first convolution layer, the horizontal Sobel convolution kernel is the same as the second convolution layer, and the vertical Sobel convolution kernel is the same as the second convolution layer. After convolving 3 second ReLU images, 15 convolutions are formed. In the third pooling layer, the image is converted into a 22 × 4 dimension image by 2 × 2 maximum pooling, and via the Softplus function in the third ReLU layer, the third ReLU layer uses the same Softplus as the first ReLU layer function to perform the thinning operation on the pooled image in the third pooling layer.

The result in the third ReLU layer is three processed images.

The convolutional kernels of the third convolutional layer are shown in FIGURE 10.

Fourth step: The image of the third ReLU layer is input into the image-processing layer. The purpose of the image-processing layer is to sharpen the edges of the image and enhance the local image contrast. An 8-neighborhood convolution operator with a center of 9 is used to convolve the image. A neighborhood convolution operator with a center of 9 is shown in Figure 11.

The image processed by the image is converted into an 11 × 2 dimension image by 2 × 2 maximum pooling. With

-1	-1	-1
-1	9	-1
-1	-1	-1

FIGURE 11. Convolutional kernels of the fourth convolutional layer.

a total of 15 images, the average gray value of the 15 images is read and input into the expanded layer, and the image is converted into the number data; the result of the expanded layer is 15 numbers, and the 15 numbers are the expanded parameters of an iris image.

The expanded parameters of three images are calculated. Three sets of expanded parameters consisting of 15 numbers can be obtained. The average of the three numbers at the same position in the three sets as that of the image's recognition parameters is calculated. The recognition parameters consist of 15 numbers.

2) ENTROPY FEATURE NEURAL NETWORK RECOGNITION AND FEEDBACK LEARNING MECHANISM

After obtaining the recognition parameters, according to the iris training samples, it is necessary to set the category labels of different categories and set the number of training irises to m. Because these images are all iris components, the identified recognition parameters can represent the iris feature. The steps for iris recognition are given as follows:

1. Set the iris information entropy and recognition parameter labels: Calculate the average value L_i of the recognition parameters of each training iris (the average value of the *i-th* recognition parameter in the training iris), calculate the probability p_i that the *i-th* recognition parameter is less than L_i in all training images, and calculate the information entropy of each recognition node under different conditions according to Formula 2.

$$\begin{aligned} H1_i &= -p_i \times \log(p_i) \\ H2_i &= -(1-p_i) \times \log((1-p_i)) \end{aligned} \tag{2}$$

where $H1_i$ represents the information entropy with the recognition parameter less than L_i, and $H2_i$ represents the information entropy with the recognition parameter greater than L_i. Finally, $H1_i \times p_i + H2_i \times (1-p_i)$ is used as the category label of the iris.

2. Calculate the matching value *HD* between the template feature information and test feature information: The objective of the recognition function is to find a category with sufficient discrimination and move the test iris feature as close as possible to the category label and observe whether it matches.

We set each recognition parameter of the test iris to f_i (*i-th* recognition parameter) and calculate the information offset Z_i of the recognition parameter according to Formula 3;

$$Z_i = \begin{cases} \dfrac{f_i}{L_i} \times H2_i \times (1-p_i) & f_i > L_i \\ \dfrac{f_i}{L_i} \times H1_i \times p_i & f_i \le L_i \end{cases} \tag{3}$$

where Z_i represents the deviation of the amount of information of the recognition parameters of the test iris at their respective probabilities (greater or less than the average L_i). In the ideal state, f_i and L_i should be the same, but they will definitely be different. Therefore, the information offset is obtained by multiplying the ratio by the respective probability and information entropy. Formula 4 is used to calculate the entropy feature G_t of *t-th* category, where G_t is the sum of the ratio of the information offset Z_i to the category label $H1_i \times p_i + H2_i \times (1-p_i)$ of each category. In the ideal state, Z_i should be 0.5 times $H1_i \times p_i + H2_i \times (1-p_i)$.

$$G_t = \sum_{i=1}^{15} \left| \frac{2 \times Z_i}{H1_i \times p_i + H2_i \times (1-p_i)} \right| \tag{4}$$

Although the value of the entropy feature G_t in each category of the test iris is not the same, it might be relatively similar. Therefore, the entropy feature G_t is enlarged by the exponential function based on e to form the category label S_t. Based on statistical ideas, we summarize the expanded scope of the category labels in each category. Because this article focuses on lightweight iris recognition, even if we apply the multi-range setting of category labels, it can also ensure that different iris categories can be well distinguished. In Formula 5, $[\alpha 1_t, \beta 1_t] \cdots [\alpha n_t, \beta n_t]$ represents different category label ranges (the interval between each interval range is set to $\lambda_1, \ldots, \lambda_n$. these values are not necessarily the same, and they are set based on the number of irises and the resulting distribution. The entropy feature G_t of the iris in *t-th* category will fall in the range after it is enlarged.). For entropy features that fall within this range, we multiply by 100 to expand and facilitate the calculation of matching values in the sigmoid function and enlarge the matching values of the same category.

$$\begin{aligned} S_t &= \begin{cases} 100 \times G_t & e^{G_t} \in [\alpha 1_t, \beta 1_t] \cap \cdots \cap [\alpha n_t, \beta n_t] \\ G_t & e^{G_t} \notin [\alpha 1_t, \beta 1_t] \cap \cdots \cap [\alpha n_t, \beta n_t] \end{cases} \\ HD &= \frac{1}{1+e^{-S_t}} \end{aligned} \tag{5}$$

Finally, the similarity between the test iris and each category is obtained through the matching value *HD*, and the maximum value of the matching value greater than 0.5 is used as the final identified category.

Feedback learning mechanism: The feedback learning mechanism of the recognition function is based on statistical concepts. With the increase in the number of test irises and the increase in recognition error conditions, we determine whether to adjust and modify the function parameters. Because the range of the category labels is obtained based on data distribution statistics, the feedback learning mechanism of the category labels in the recognition function

TABLE 1. The key indicators of the three devices.

	JLU-4.0	JLU-6.0	JLU-7.0
Pixel	5000000	2000000	300000
Collection distance	150-200mm	100-150mm	150-200mm
Resolution	640×480	640×480	640×480
Light	Infrared	Infrared	Non-infrared
Color	color	Grayscale	Grayscale

primarily adjusts $[\alpha 1_t, \beta 1_t] \cdots [\alpha n_t, \beta n_t]$ and the range interval $\lambda_1, \ldots, \lambda_n$ in Formula 5 based on the occurrence of recognition error conditions. At the same time, because the category labels and entropy features are calculated according to L_i and p_i, L_i and p_i are adjusted as the number of irises increases, thereby achieving dynamic learning. The entropy feature of the function and the range of the category labels can be dynamically adjusted with the increase of the number of irises, thereby achieving the current optimal effect.

III. EXPERIMENTS AND ANALYSIS

Experimental Data: All experiments in this paper use the JLU-4.0 (device in Figure 1b), JLU-6.0 (device in Figure 1d), and JLU-7.0 (device in Figure 1f) iris libraries [27]. The JLU-6.0 iris library is a low-end acquisition device, JLU-4.0 and JLU-7.0 are advanced devices. As of 2020, the JLU-6.0 original iris library contains more than 100 categories of irises, and each category contains more than a thousand unstable irises photographed in various states (including the standard morphology set). The JLU-4.0 original iris library contains more than 50 categories of iris, and each category has thousands of unstable irises photographed in various states (including the standard morphology set). The JLU-7.0 original iris library has more than 30 categories of iris, and each category has more than a thousand unsteady irises (including standard morphology sets) taken in various states, and the three types of iris libraries are constantly expanding every year. The irises that meet the prerequisites of the algorithm are selected from the original library and directly mixed, without distinguishing according to the state, to form an experimental iris library. The key indicators of the three devices are shown in TABLE 1.

Experimental Setup: In these experiments, the computing system includes a dual-core 2.5 GHz CPU with 8 GB memory, and the operating system is Windows.

Section 3.1 gives an explanation of the structural meaning, and the rationality and reasons of the settings of each portion of the method in this paper are explained in the form of data:

Section 3.1.1: **Constrained multi-state iris recognition and feature discrimination.** Iris recognition is performed binary matching shown in the example. Analysis based on experimental results shows the impact of the constrained multi-state iris on heterogeneous iris recognition and highlights the rationality of the prerequisite research in this paper.

Section 3.1.2: **Feature correlation and significance of recognition function.** This section numerates the entropy features and entropy expansion values under different numbers of categories, explains the discrimination between different features, shows that the final feature representation of this article can represent the characteristics of the iris, and finally explains the significance of the iris recognition function.

Section 3.1.3 **Reasonable setting of feedback learning mechanism**. This section lists the accuracy of different numbers of irises under the lightweight training data, enumerates the average and probability values of different iris numbers (as well as the distribution of the category label range), and explains the significance of setting up a feedback learning mechanism for the optimization of recognition module.

Section 3.2 describes the method and performance of the experiment to clarify the performance of the algorithm:

Section 3.2.1: **Heterogeneous versatility experiment**. The same type of certification experiments are performed via three iris libraries to verify the universality of the overall structure of the method proposed in this paper for heterogeneous recognition. Section 3.2.2: **Recognition performance experiment**. After confirming that the quality has no effect on iris recognition, the performance of the recognition function in recognition is divided into three main components: 1. Single-category certification experiment: Different irises are used to match a single category, and the performance of single category recognition is judged by the ROC curve; 2. Multi-category recognition experiment: Multi-category recognition performance is judged via common recognition of the multi-category iris; 3. Addition of new category recognition experiment: This section verifies how the system maintains the advantages of recognition after addition of a new category based on the original recognition structure. Section 3.2.3: **Structural properties and algorithm independence.** The rationality of the structure design of this paper is indicated by replacing the algorithms in the recognition method and not using feature fusion.

Section 3.3 contains a comprehensive experiment. Under the prerequisites of this paper, the combination of the recognition structure of this paper and the existing recognition algorithm is compared to illustrate the advantages of this algorithm compared with the current algorithm.

A. EXPLANATION OF STRUCTURAL MEANING

1) CONSTRAINED MULTI-STATE IRIS RECOGNITION AND FEATURE DISCRIMINATION

Experimental Setup in This Section: In this section of the experiment, each iris library uses 30 categories (each of which has 10 images; the images are not classified in advance and are randomly mixed) and a total of 300 images. The iris image is transformed into a 178 × 30 dimension binary feature code by an 8-neighborhood LBP operator [28]. The irises of the same category in the same iris library are matched with each other, and the impact of the unsteady iris on iris recognition is analyzed by the Hamming distance [29]. In each iris library, the number of comparisons in the same category is 100, and the number of comparisons in different

TABLE 2. Example of data for Hamming distance in three libraries.

No.	JLU-4.0	JLU-6.0	JLU-7.0
1	0.469618	0.500347	0.500694
2	0.465972	0.517187	0.502951
3	0.461979	0.512153	0.512554
4	0.477083	0.498264	0.501562
5	0.460069	0.515799	0.493403
6	0.463542	0.509201	0.505382
7	0.457292	0.508681	0.503646
8	0.465625	0.500347	0.452778
9	0.450868	0.517187	0.445139
10	0.472049	0.512153	0.456771
11	0.454861	0.498264	0.472917
12	0.449479	0.515799	0.500694
13	0.465104	0.509201	0.502951
14	0.459896	0.469618	0.525545
15	0.466319	0.471354	0.480035
16	0.501042	0.469618	0.471701
17	0.499826	0.457465	0.474653
18	0.488715	0.462674	0.459896
19	0.496528	0.467708	0.476215
20	0.490972	0.469618	0.480035

categories is 200. The Hamming distance distribution of the same category and different categories is used to illustrate the impact of the unsteady-state iris on heterogeneous iris recognition.

A list of selected Hamming distance data in the three libraries (Nos. 1-10 in each library are Hamming distances of the same category, and Nos. 11-20 are Hamming distances of different categories) is shown in TABLE 2. The distribution map of 300 Hamming distances in the three libraries is shown in FIGURE 12 (100 red dots (numbers 1-100), which represent the Hamming distance value of the same category of iris, and 200 blue dots (numbers 101-300), which represent different Hamming distance values of the different categories of iris). The abscissa (x-axis) represents the image serial number, and the ordinate (y-axis) represents the Hamming distance value.

As a type of iris recognition method for large differences, the LBP operator and Hamming distance are suitable for showing the relative changes between different features. As shown in TABLE 2 and FIGURE 12, although the iris libraries are not the same, the Hamming distances caused by binary coding of the multi-state irises in different states in the three libraries through LBP are all concentrated in the interval [0.4, 0.6]. No major differences are noted between the same category and different categories because under the multi-state iris, the shooting state between the test iris and the template iris cannot be predicted. The visual difference between the two irises is large, the gray difference between the irises in the same area might change or even reverse, and the relative difference features are not reliable. In this case, it is highly important to extract the absolute differences between the iris features (highly differentiated features), and in the case in which the requirements for the amount of data and data classification cannot be met, it is also necessary to design different acquisitions for the multi-state iris. Therefore, research on the constrained multi-state iris and heterogeneous recognition has practical significance.

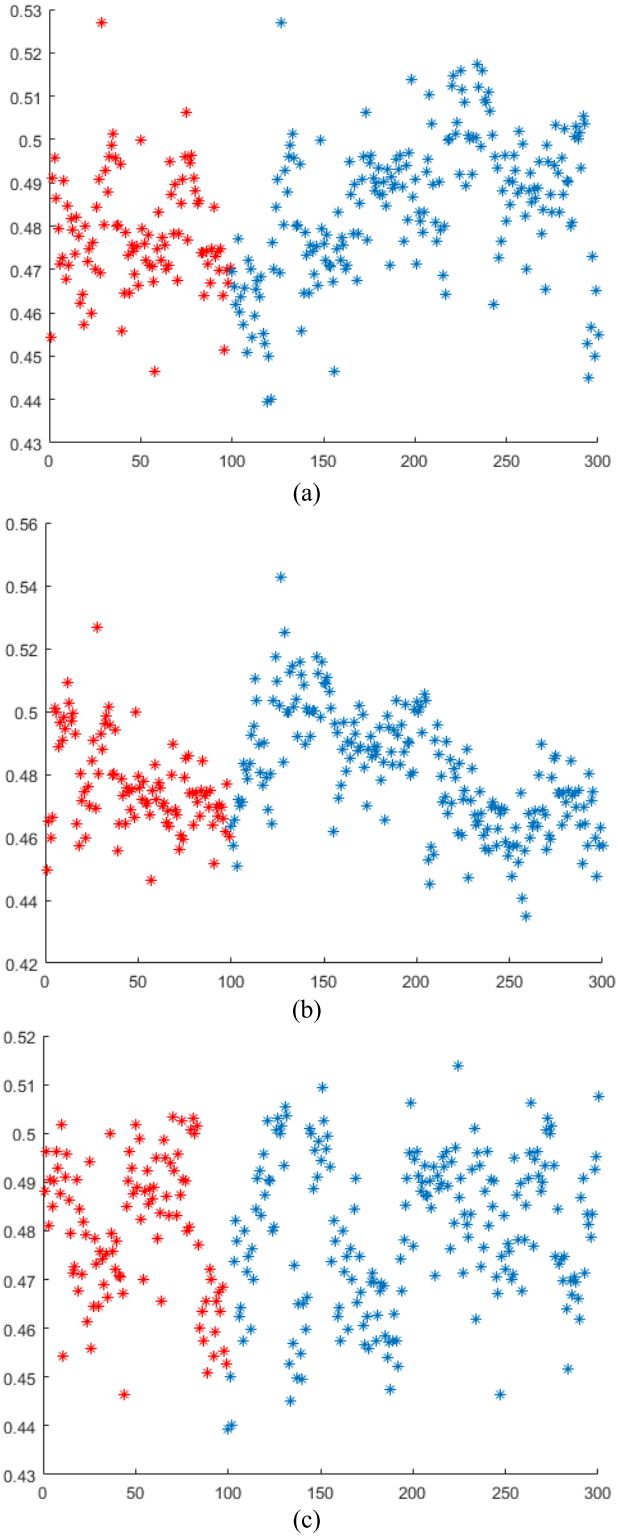

FIGURE 12. The distribution map of 300 Hamming distances in the three libraries (a) 4.0, (b) 6.0, (c) 7.0.

2) FEATURE CORRELATION AND SIGNIFICANCE OF RECOGNITION FUNCTION

Experimental Setup in This Section: In this section of the experiment, after confirming that the quality evaluation has no effect on iris recognition, three categories are selected from each iris library, and each category contains 500 training irises (random collection, no prior classification, and for the multi-source features in the experiment, Gaussian filtering (smoothed) and equalizing histogram (highlighted) are used as image-processing algorithms.). We test one iris (same equipment and training environment as the iris) and use the recognition function designed in this paper for iris recognition. According to the average recognition parameter L_i of the training iris, the probability that the *i-th* recognition parameter p_i in all training images is less than L_i, the entropy feature G_t, the expansion value e^{G_t}, the feature correlation analysis and the analysis of the recognition function design are explained. It can be used to represent the unique features of the iris and to determine how effectively the function performs multi-category recognition.

TABLE 3 shows an example of the L_i and p_i of 15 recognition parameters obtained from 500 training irises in one category in each library. TABLE 4 shows examples of the entropy features G_t and the expansion values e^{G_t} obtained from the recognition functions corresponding to the tags in the three iris images (each iris library lists 3 categories, and each category lists 1 image). Based on the enlarging value of the entropy feature when comparing the same category of each iris library in TABLE 4 (bold font in TABLE 4), 1000 images are randomly selected from the three categories of each iris library. The multiple distribution between the expansion value and the base value obtained when the categories are compared with the recognition functions of different categories is shown in FIGURE 13.

The clustering effect between the same category and different categories is analyzed in FIGURE 13. In FIGURE 13, the abscissa represents the sequence of events compared, where 1 represents the iris in category 1 for contrast matching using the recognition function of the category label of category 1, 2 represents the iris in category 2 for contrast matching using the recognition function of the category label of category 1, 3 represents the iris in category 3 for contrast matching using the recognition function of the category label of category 1, 4 represents the iris in category 1 for contrast matching using the recognition function of the category label of category 2, 5 represents the iris in category 2 for contrast matching using the recognition function of the category label of category 2, 6 represents the iris in category 3 for contrast matching using the recognition function of the category label of category 2, 7 represents the iris in category 1 for contrast matching using the recognition function of the category label of category 3, 8 represents the iris in category 2 for contrast matching using the recognition function of the category label of category 3, and 9 represents the iris in category 3 for contrast matching using the recognition function of the category label of category 3.

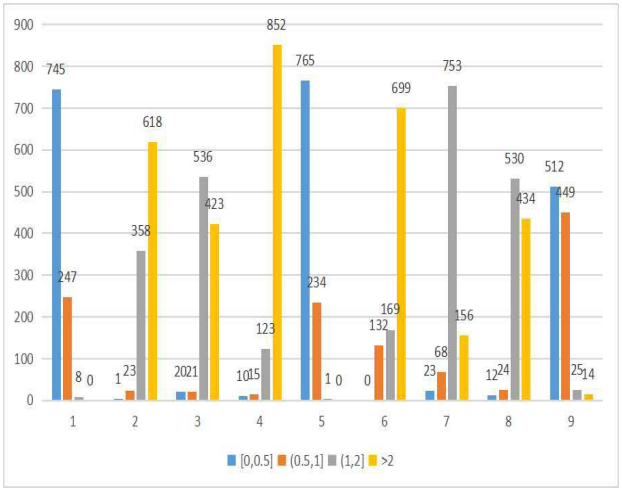

(a)

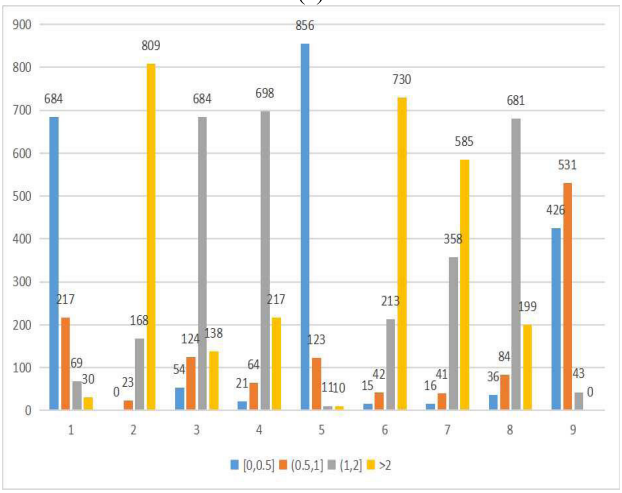

(b)

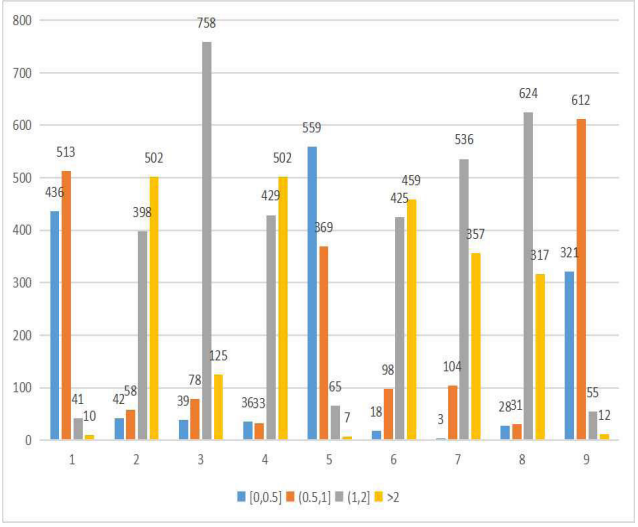

(c)

FIGURE 13. Distribution of multiples between enlarged and base values in three libraries (a) 4.0, (b) 6.0, (c) 7.0.

In FIGURE 13, the ordinate represents the number of irises. The four bar lines represent the multiples between the enlarged value and the base value obtained when testing and

TABLE 3. The example of L_i and p_i of 15 recognition parameters.

		JLU-4.0	JLU-6.0	JLU-7.0
1	L_i	44.5697	18.7266	24.374
	p_i	0.6	0.54	0.58
2	L_i	19.8304	33.2394	67.3079
	p_i	0.6	0.56	0.48
3	L_i	10.2241	24.4030	49.4673
	p_i	0.6	0.66	0.5
4	L_i	48.3454	22.4709	32.8769
	p_i	0.4	0.52	0.48
5	L_i	35.5758	39.0133	54.8345
	p_i	0.4	0.56	0.42
6	L_i	13.4000	31.9861	55.0618
	p_i	0.6	0.6	0.46
7	L_i	45.9515	20.8782	25.9436
	p_i	0.6	0.5	0.58
8	L_i	19.2727	29.8964	52.7546
	p_i	0.4	0.54	0.54
9	L_i	13.9576	18.9630	38.4412
	p_i	0.6	0.62	0.54
10	L_i	37.4303	19.3818	21.1418
	p_i	0.4	0.52	0.52
11	L_i	18.5212	26.3140	50.537
	p_i	0.6	0.64	0.44
12	L_i	15.4909	17.6794	34.1182
	p_i	0.6	0.58	0.52
13	L_i	44.9637	23.6218	31.3618
	p_i	0.4	0.58	0.48
14	L_i	25.9758	37.8012	50.7218
	p_i	0.8	0.56	0.48
15	L_i	13.7091	28.5770	54.723
	p_i	0.6	0.64	0.36

TABLE 4. Entropy features in three libraries and their enlarged values.

			Category 1	Category 2	Category 3
JLU-4.0	Category 1	G_t	**13.6251**	10.9602	11.8972
		e^{G_t}	**826655**	57535.2	146855
	Category 2	G_t	13.6057	**12.9352**	11.1242
		e^{G_t}	810701	**414669**	67793.8
	Category 3	G_t	13.0231	13.1033	**11.9808**
		e^{G_t}	452757	490549	**159665**
JLU-6.0	Category 1	G_t	**13.3372**	9.37611	11.5594
		e^{G_t}	**619816**	11803	104758
	Category 2	G_t	10.8608	**11.5123**	8.37192
		e^{G_t}	52095	**99941.9**	4323.92
	Category 3	G_t	13.525	10.8111	**12.9036**
		e^{G_t}	747886	49569.1	**401766**
JLU-7.0	Category 1	G_t	**12.4273**	10.2652	11.6807
		e^{G_t}	**249515**	28715.8	118265
	Category 2	G_t	10.3793	**13.5558**	9.64025
		e^{G_t}	32186.7	**771261**	15371.2
	Category 3	G_t	9.98933	11.9891	**13.0538**
		e^{G_t}	21792.8	160987	**466869**

TABLE 5. Examples of the entropy feature G_t and the expansion value e^{G_t}.

		JLU-4.0	JLU-6.0	JLU-7.0
1	G_t	13.2344	11.7369	12.2545
	e^{G_t}	559271	125107	209926
2	G_t	13.9789	11.1458	13.1756
	e^{G_t}	1177450	69274.6	527353
3	G_t	13.3944	11.9027	13.4839
	e^{G_t}	656330	147669	717775
4	G_t	13.5536	12.2851	13.1123
	e^{G_t}	769614	216449	495014
5	G_t	11.7526	11.3628	13.461
	e^{G_t}	127081	86058.2	701491
6	G_t	13.7969	12.5639	13.2412
	e^{G_t}	981518	286040	563067
7	G_t	13.7253	11.902	13.8118
	e^{G_t}	913733	147556	996324
8	G_t	13.3992	10.6465	13.0529
	e^{G_t}	659478	42044.4	466445
9	G_t	13.7427	11.0589	13.2532
	e^{G_t}	929806	63506.7	569881
10	G_t	13.1547	10.3877	13.3031
	e^{G_t}	516454	32458.6	599077

comparing the recognition functions of the same category and different categories. Among them, [0, 0.5] represents 0 to 0.5 times the base value when the expanded value is tested, (0.5, 1] represents 0.5 to 1 times the base value when the expanded value is tested, (1, 2] represents 1 to 2 times the base value when the expanded value is tested, and >2 represents more than 2 times the base value when the expanded value is tested. The numbers on the bars represent the values of the bars.

Examples of the entropy feature G_t and the expansion value e^{G_t} obtained from the same category of randomly selected multiple images in three libraries (each library uses 10 images as an example) are shown in TABLE 5.

Because no standard definition of iris characteristics currently exists, the correlation of iris characteristics in this paper is based on two main indicators: uniqueness and discrimination. Therefore, the analysis is based on TABLE 3,TABLE 4 and TABLE 5. From the recognition function designed in this paper, it can be observed that because the iris is multi-state, after the convolutional operation, there are no identical recognition parameters. As the iris is trained, with different numbers and the establishment of a feedback mechanism, L_i and p_i of the 15 recognition parameters are also constantly changing. Therefore, the iris parameters are different between

different categories of different images. The data representing the iris are unique and can be used as the iris features, and because of the multiple states of the iris, the difference in feature parameters between the selected images is low. Therefore, the purpose of the recognition function in this paper is to improve the discrimination of the iris feature data for recognition.

It can be observed from FIGURE 13 that when the recognition function of the same category is used as a reference recognition function, the clustering effect between the same category and different categories is different. The difference between multi-category recognition and single authentication is that different types of iris data in multi-category recognition experiments must be calculated by the same recognition function to find the best matching value. In other words, the recognition function based on one category can effectively distinguish it from the corresponding category when passing through the recognition parameters of another category. In the prerequisites of this paper, the number and classification requirements of the iris dataset are far from the requirements of deep learning, and thus, the conventional large-scale deep learning architecture with dozens or even hundreds of layers finds it difficult to function. The lightweight neural network architecture is limited by the convergence of the excitation function, and thus, the recognition function is designed based on the iris features. The design concept of the recognition function is that the iris feature data cannot be changed after the feature extraction method is fixed. We adjust the internal parameters of the recognition function to ensure that the discrimination between the same category and different categories is as wide as possible.

It can be observed from TABLE 4 that the recognition functions based on a certain category show certain differences in entropy features when passing through different categories of data. The data in TABLE 5 show that the data difference between the same category is small, and closer clustering can be achieved. However, due to the limitation of the number of recognition parameters, the difference in entropy features is not obvious in certain cases. Therefore, the exponential function with the base e is expanded to expand the value of the entropy features, thus greatly expanding the differentiation among the categories of iris and the performance of multi-category recognition. Based on analysis of the data in TABLE 5 and FIGURE 13, the entropy features of the iris in the same category are mostly concentrated in a certain region. After expansion, due to the multi-state iris, the enlarged iris image is concentrated in different regions. Even if the entropy features are relatively close, they can be expanded to a large gap. Because the prerequisites for this paper require running the tester to retake the iris image, this paper uses the multi-range method. Using reasonable range intervals, the enlarged data of different categories of iris after the same category label can be effectively distinguished and will not coincide. This result can greatly improve the accuracy of multi-classification.

TABLE 6. Feedback and updates.

Case	Training iris number	Test iris number	Number of correct recognition	Correct recognition rate	Whether to update judgment
			JLU-4.0		
1	10	50	48	96%	No
2	10	100	69	69%	Yes
3	100	200	189	94.5%	Yes
4	500	200	200	100%	No
			JLU-6.0		
1	10	50	38	76%	Yes
2	100	200	193	96.5%	No
3	100	500	375	75%	Yes
4	500	500	499	99.8%	No
			JLU-7.0		
1	10	50	42	84%	Yes
2	50	100	89	89%	Yes
3	200	200	198	99%	No
4	200	500	423	84.6%	Yes

3) REASONABLE SETTING OF FEEDBACK LEARNING MECHANISM

Experimental Setup in This Section: After ensuring that the quality of the iris does not affect the recognition results, each iris library selects one category and uses the recognition function designed in this paper for iris recognition. The growth trend of 200 test irises (experimental test images and training images) without a feedback mechanism when the training irises consist of 10, 100, 200, and 500 images in the three iris libraries is presented in FIGURE 14.

In FIGURE 14, the abscissa represents the serial number of the test image, and the ordinate represents the number of irises recognized correctly. The feedback learning mechanism is used to dynamically modify the recognition function (the average L_i and probability values p_i of the recognition parameters and the range of the category interval). Each of the three iris libraries selects a certain category of iris. TABLE 6 shows examples of different amounts of training, number of iris recognitions, and updated examples of the recognition situation. This paper assumes that if the correct recognition rate is less than 95% or if the number of trained irises is increased by more than 5 times (where the new training iris contains the previous test iris), then the model needs to be updated.

Although the design of the recognition function guarantees the accuracy of the iris multi-classification results, it can be observed from FIGURE 14 that when the number of trained irises is small and constant, if the number of tested irises is much larger than the number of trained irises, the accuracy rate is expected to decrease. Because the number of training irises is insufficient to make the selected category label range insufficient, the information entropy value cannot be guaranteed to be always available. Therefore, it is necessary to increase the training data in time to adjust the recognition model, but the user needs to know when the recognition model needs to be adjusted to avoid unnecessary adjustment. Thus, it is necessary to design a feedback learning mechanism.

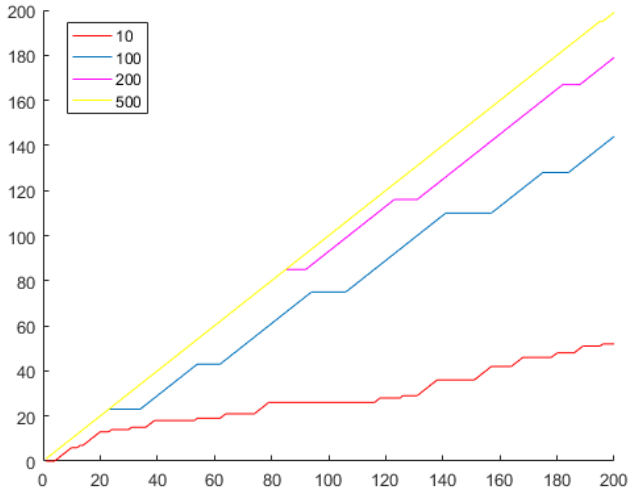

(a)

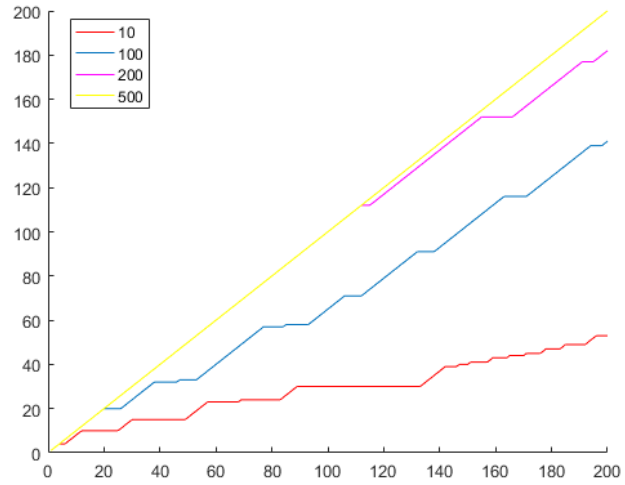

(b)

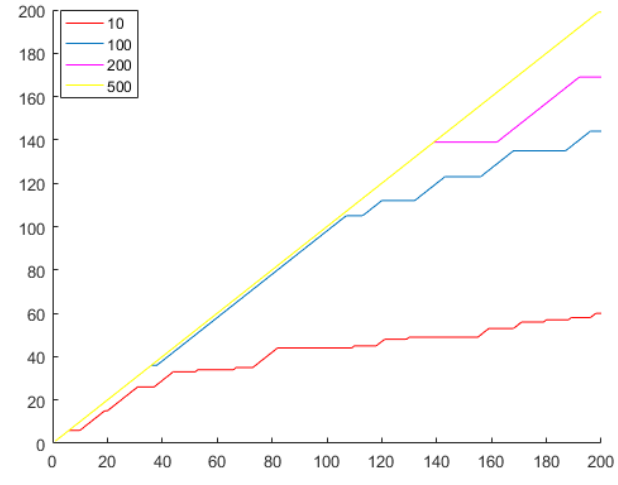

(c)

FIGURE 14. The growth trend of 200 test irises, (a) 4.0, (b) 6.0, (c) 7.0.

In the example of the feedback learning mechanism shown in TABLE 6, it can be observed that the number of irises trained affects the accuracy of the large-scale test iris, and thus, dynamic adjustment is necessary. The number of training irises should ensure the correct recognition rate of the test iris within a certain number, and the designed feedback learning mechanism can prompt the user to increase the training iris data and adjust the new recognition model (adjust the average number and concept, add new category interval ranges) such that the recognition model always maintains a high accuracy rate and makes up for the problem of the dynamic adjustment of the convolutional neural network structure under the training of lightweight data.

TABLE 7. Test results of heterogeneous universal experiments.

		The number of iris acquisitions	false rejection	false acceptance
JLU-4.0	Category 1	305	5	0
	Category 2	300	0	0
	Category 3	303	2	1
	Category 4	307	6	1
	Category 5	304	4	0
JLU-6.0	Category 1	305	5	0
	Category 2	300	0	0
	Category 3	300	0	0
	Category 4	301	0	1
	Category 5	301	1	0
JLU-7.0	Category 1	300	0	0
	Category 2	302	2	0
	Category 3	300	0	0
	Category 4	300	0	0
	Category 5	303	1	2

B. RECOGNITION METHOD PERFORMANCE EXPERIMENT

1) HETEROGENEOUS VERSATILITY EXPERIMENT

Experimental Settings and Indicators: In this section of the experiment, each of the three iris libraries uses five categories as the verification data, and the parameters of each category are trained by 500 training images qualified by the quality evaluation system (without new feedback learning adjustments). In multi-category recognition for each category for separate collection tests, each category directly collects one iris for individual matching. The tester's iris was collected with the guidance of posture correction and normal shooting. Iris quality assurance has no effect on recognition. Multi-category recognition of the five categories of the same iris library are selected for comparison. For the multi-source features in the experiment, Gaussian filtering (smoothed), and the equalized histogram (highlighted) are used as the image-processing algorithms. The judgment indicators for the results of this experiment are listed as follows:

1. Number of iris acquisitions when each category of the iris library reaches 300 accurate recognitions (including the case in which the tester is re-taken to achieve accuracy, i.e., false rejection).
2. Each category of each iris library reaches 300 iris recognition errors (false acceptance) when the recognition is accurate.

The test results are shown in TABLE 7.

It can be observed from TABLE 7 that in the process of iris recognition using the same set of recognition models by

multiple iris libraries, the error acceptance rate of the iris is notably low, the occurrence of false acceptance is rare, and the number of false rejections is also within the scope of human tolerance. This result occurs because the parameters in the iris recognition function are based on the training iris, and the multi-category features are greatly diluted by the entropy feature expansion effect, thereby increasing the possibility of parameter values crossing between different categories. Different categories are distinguished by the range interval, and the range of further dilution of the recognition function feature values is narrowed to increase the matching value of the same category as much as possible and to reduce the matching value of different categories. In addition, although notably few cases of erroneous acceptance occur, the feedback learning mechanism of this paper can make feedback adjustments for new situations, adjust the problems in the recognition structure in time, and improve the recognition rate.

It can be concluded from this experiment that the recognition structure designed in this paper can effectively operate in different iris libraries, has good heterogeneity and universality, and can effectively operate in multiple iris libraries.

2) RECOGNITION PERFORMANCE EXPERIMENT

Experimental Indicators: The multi-source features in the recognition performance experiments use Gaussian filtering (smoothing) and the equalization histogram (prominence) as multi-source image-processing algorithms. The evaluation indicators include correct recognition rate (CRR) [42] and ROC space (curve) (including true positive (TP), false positive (FP), true negative (TN), false negative (FN), false positive rate (FPR), true positive rate (TPR), accuracy (ACC), and area under curve (AUC)) [43]. The ROC space (curve) defines the false positive rate (FPR) as the x-axis and the true positive rate (TPR) as the y-axis. Because the prerequisite requirement for this article is to guarantee accuracy and allow users to re-shoot, the case of false rejection is also considered true. In the experiment described in this section, the definition of each indicator is given as follows:

True positive (TP): The actual category is 1, and the actual output is 1, which represents the conclusion that the image of category A of the experimental iris library is considered to belong to category A or not belong to the experimental iris library.

False positive (FP): The actual category is 1, and the actual output is 0, which represents the conclusion that the image of category A of the experimental iris library is considered to not belong to category A.

True negative (TN): The actual category is 0, and the actual output is 0, which represents the conclusion that the image does not belong to category A of the experimental iris library and is considered to neither belong to category A nor any other category.

False negative (FN): The actual category is 0, and the actual output is 1, which represents the conclusion that the image does not belong to category A of the experimental iris library and is considered to belong to category A or another category in the iris library.

TABLE 8. Recognition times of each category in different iris libraries.

		The same category	Different category
JLU-4.0	Category 1	1745	9584
	Category 2	1695	9358
	Category 3	1869	9756
	Category 4	1856	9865
	Category 5	1985	9435
JLU-6.0	Category 1	1869	9458
	Category 2	1985	9256
	Category 3	1573	9356
	Category 4	1869	9875
	Category 5	1746	9635
JLU-7.0	Category 1	1698	9125
	Category 2	1896	9357
	Category 3	1763	9514
	Category 4	1658	9341
	Category 5	1698	9465

1. Single-classifier Certification Experiment

Experimental Setup in This Section: In this section, each of the three iris libraries is selected from five categories for experimentation, and the parameters of each category are trained from 2000 training images qualified for quality evaluation (without new feedback learning adjustments). The source features are Gaussian filtered (smoothed), and the equalized histogram (highlighted) is applied as image-processing algorithms. During the test, the same category and different categories are used in single-class recognition (originating from the same iris library, and the test iris and training iris are different). We observe the experimental data for analysis. TABLE 8 shows the recognition times of each category in different iris libraries. TABLE 9 shows the partial correspondence between FPR and TPR in a single classifier of each category of different iris libraries. The threshold range of the ROC curve in this experiment is [0.5, 1], and the interval is 0.01.

The ROC curves for single-category recognition of each category in the three iris libraries are shown in FIGURE 15.

From FIGURE 15, under the condition that the number of training irises is guaranteed, although the certification effect of each category of different iris libraries is different, the overall area under the curve (AUC) is significantly larger than 0.5, indicating that each The accuracy of single-category certification of each category is high, and the method has good heterogeneity. If the amount of data is sufficient, the method has good predictive value.

According to analysis of the results in TABLE 9 and FIGURE 15, due to the unpredictability of the multi-state iris, the feature appearance between different iris images might be notably different, which is reflected probabilistically in the amplitude value and distribution after edge detection based on the limitation of the scale and situation classification of the iris data set, which makes it impossible to use a large-scale deep learning architecture. The recognition function of the method in this paper is based on the current iris data when

TABLE 9. Partial correspondences between FPR and TPR.

JLU-4.0	Category 1	FPR	0.0535118	0.113989	0.137772	0.24565
		TPR	0.140741	0.964408	0.977589	0.999995
	Category 2	FPR	0.0623851	0.0780048	0.16875	0.19545
		TPR	0.363784	0.581086	0.97454	0.984536
	Category 3	FPR	0.065851	0.090945	0.0952569	0.1450997
		TPR	0.423784	0.893238	0.930528	0.989536
	Category 4	FPR	0.0740588	0.088542	0.0995454	0.1305897
		TPR	0.78086	0.882546	0.9725859	0.9898536
	Category 5	FPR	0.0615118	0.071851	0.1263959	0.152097
		TPR	0.180741	0.52574	0.960505	0.9808536
JLU-6.0	Category 1	FPR	0.0528719	0.0750997	0.0796357	0.124879
		TPR	0.750628	0.913536	0.923448	0.97955
	Category 2	FPR	0.0460048	0.0668532	0.0910997	0.1216861
		TPR	0.591086	0.91109	0.963536	0.979484
	Category 3	FPR	0.0560048	0.078772	0.082738	0.1092661
		TPR	0.781086	0.939589	0.94675	0.979484
	Category 4	FPR	0.0520048	0.0897772	0.093738	0.1506861
		TPR	0.731026	0.947589	0.95454	0.991404
	Category 5	FPR	0.056268	0.0688719	0.0950997	0.11568
		TPR	0.9396	0.948428	0.983536	0.989456
JLU-7.0	Category 1	FPR	0.015374	0.025645	0.065745	0.134146
		TPR	0.7661404	0.903	0.965	0.9953789
	Category 2	FPR	0.006946	0.007423	0.02641	0.085256
		TPR	0.555065	0.625082	0.942664	0.97568
	Category 3	FPR	0.002658	0.0092447	0.015256	0.057254
		TPR	0.4386	0.891523	0.958829	0.965126
	Category 4	FPR	0.00489	0.0152447	0.035143	0.046246
		TPR	0.49854	0.899523	0.936598	0.955326
	Category 5	FPR	0.00232	0.008758	0.035155	0.115756
		TPR	0.21568	0.7950455	0.958829	0.982545

performing single-category recognition. The same category labels and recognition parameters are clustered in the same category, and the parameters are differentiated according to the probability of different amplitude values. Features are extracted in the form of information entropy to find the connection between the images of the same category to the extent possible. Iris features of the same category can be grouped together such that features of different categories

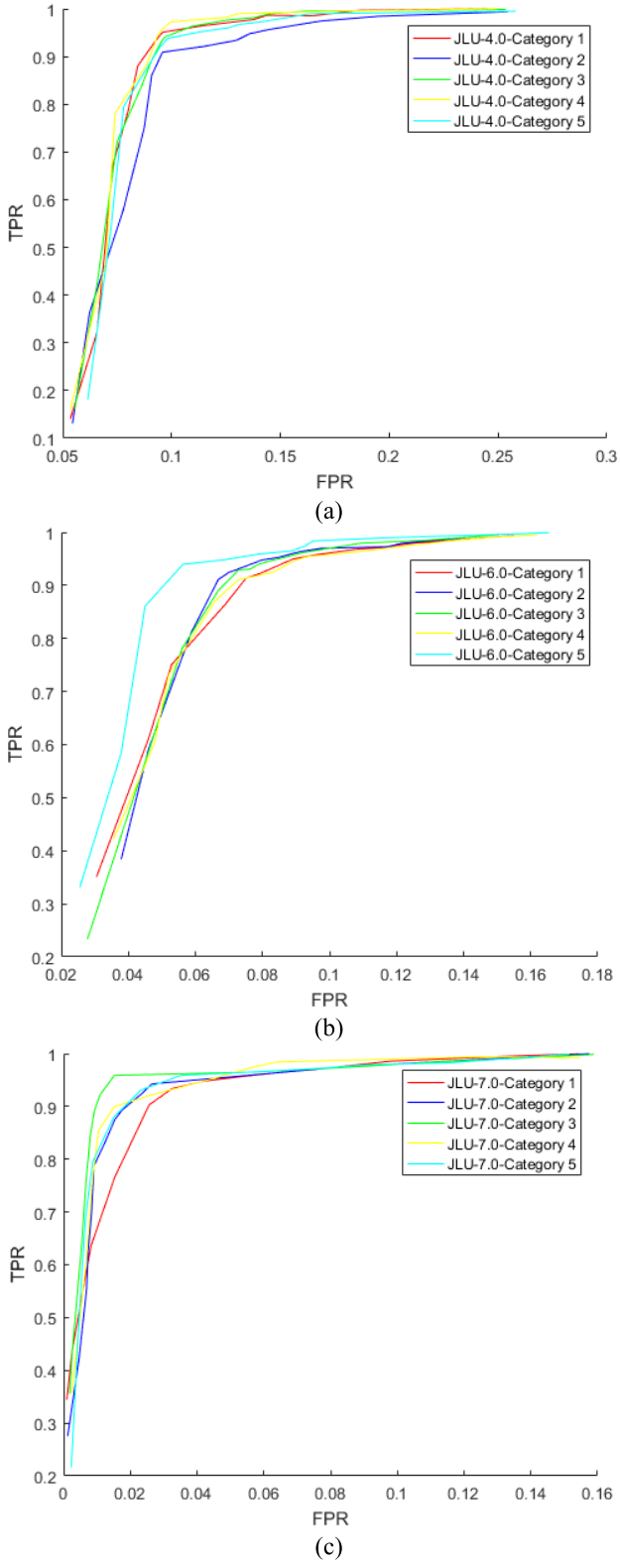

FIGURE 15. The ROC curves of single-category recognition of each category of the three iris libraries, (a) 4.0, (b) 6.0, (c) 7.0.

cannot be aggregated. In expanding and diluting the non-linear function, the clusters of the same category in the multi-state iris are strengthened by setting multiple label ranges.

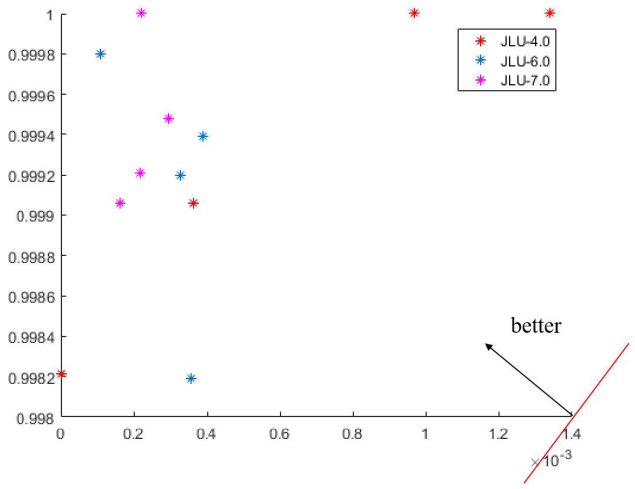

FIGURE 16. The spatial distribution of TPR and FPR of the multi-category data.

Compared with the mechanical single threshold judgment, the recognition range is larger, and the structure setting is more flexible.

2. Multi-category Recognition Experiment

Experimental Setup in This Section: In this section experiment, the number of iris categories in each of the three iris libraries is set to 5, 10, 15, and 20. Each category has 2000 initial training irises (the quality evaluation index is the evaluation index exemplified in this paper). After the experiment is completed, if the number of categories is small, all test irises are converted to new training irises, and new categories of irises are added. The recognition model is optimized by feedback, and the parameters in the recognition function are adjusted. The test iris and training iris of each category experiment are different irises taken in the same state, which meets the prerequisites of this article and excludes extreme interference. The irises in the comparison are all irises inside the experimental iris bank. For the multi-source features in the experiment, Gaussian filtering (smoothed) and the equalizing histogram (highlighted) are used as image-processing algorithms.

The comparison times and recognition of the four comparison experiments in JLU-4.0 are shown in TABLE 10. The comparison times and recognition of the four comparison experiments in JLU-6.0 are shown in TABLE 11. The comparison times and recognition of the four comparison experiments in JLU-7.0 are shown in TABLE 12. The TPR, FPR and ACC of the three iris libraries are shown in TABLE 13. The spatial distribution of TPR and FPR of the multi-category data from different iris libraries is shown in FIGURE 16.

The results in tables 10-13 and FIGURE 16 show that the multi-classification results in the three iris libraries are better and that the method has good heterogeneity. The design of the recognition function can effectively improve the output results of the same category, suppress the output results of different categories, and also effectively distinguish the outer iris

TABLE 10. The number of comparison times and recognition situation of JLU-4.0.

The number of categories is 5		The actual output		Total
		1	0	
The actual category	1	558	0	558
	0	1	896	897
Total		559	896	1455
The number of categories is 10		The actual output		Total
		1	0	
The actual category	1	1068	2	1070
	0	0	1489	1489
Total		1068	1491	2559
The number of categories is 15		The actual output		Total
		1	0	
The actual category	1	1658	2	1660
	0	0	2045	2045
Total		1658	2047	3705
The number of categories is 20		The actual output		Total
		1	0	
The actual category	1	2142	1	2143
	0	2	2743	2745
Total		2144	2744	4888

TABLE 11. The number of comparison times and recognition situation of JLU-6.0.

The number of categories is 5		The actual output		Total
		1	0	
The actual category	1	1653	2	1655
	0	1	5123	5124
Total		1654	5125	6779
The number of categories is 10		The actual output		Total
		1	0	
The actual category	1	3324	4	3328
	0	6	11235	11241
Total		3330	11239	14569
The number of categories is 15		The actual output		Total
		1	0	
The actual category	1	5026	2	5028
	0	1	18695	18696
Total		5027	18697	23724
The number of categories is 20		The actual output		Total
		1	0	
The actual category	1	6235	7	6242
	0	5	21368	21373
Total		6240	21375	27615

category. Because of the unpredictability of the multi-state iris, the effect of edge detection based solely on convolutional kernels can improve the uniqueness of a single category of iris features, and through analysis of a large number of training category label data, we can find data clustering regions to ensure the accuracy of single category recognition. However, in the case of multi-classification, the influence of feature discrimination is more important, and the edge portions of the category label clustering regions between multiple features must be prevented from overlapping. Therefore, dilution of the cluster area and clarification of the edge of the cluster area is a key point.

In this method, the parameters in the recognition function are determined by the features of the training iris itself. Various irises are mixed together. Without distinguishing the states, the differences in each category of iris and each in the same category are fully considered. We identify the weight

TABLE 12. The number of comparison times and recognition situation of JLU-7.0.

The number of categories is 5		The actual output		Total
		1	0	
The actual category	1	1257	1	1258
	0	0	4527	4527
Total		1257	4528	5785
The number of categories is 10		The actual output		Total
		1	0	
The actual category	1	2542	2	2544
	0	2	9145	9147
Total		2544	9147	11691
The number of categories is 15		The actual output		Total
		1	0	
The actual category	1	3854	4	3858
	0	2	13548	13550
Total		3856	13552	17408
The number of categories is 20		The actual output		Total
		1	0	
The actual category	1	5312	3	5315
	0	5	18562	18567
Total		5317	18565	23882

TABLE 13. The TPR, FPR and ACC of the three iris libraries.

		TPR	FPR	ACC
JLU-4.0	The number of categories is 5	99.821%	0%	0.9993
	The number of categories is 10	100%	0.134%	0.9992
	The number of categories is 15	100%	0.097%	0.9995
	The number of categories is 20	99.906%	0.0364%	0.9993
JLU-6.0	The number of categories is 5	99.939%	0.0390%	0.9996
	The number of categories is 10	99.819%	0.0356%	0.9993
	The number of categories is 15	99.980%	0.0107%	0.9998
	The number of categories is 20	99.920%	0.0327%	0.9996
JLU-7.0	The number of categories is 5	100%	0.0221%	0.9998
	The number of categories is 10	99.921%	0.0219%	0.9996
	The number of categories is 15	99.948%	0.0295%	0.9996
	The number of categories is 20	99.906%	0.0162%	0.9997

difference of the parameters and represent the information in the form of information entropy. It can be observed from the single-category recognition experiment that the design concept of the recognition function uses the category labels of the same category of iris as a component of the function to gather the calculated values of the same category of iris and to distinguish the calculated values of different categories of iris to the extent possible. Because the weight of the recognition parameter impact on the recognition result and the amount of information it carries are heavily considered during the design, the results of different categories of iris are notably different via different proportions and the degree of matching to the results of the test iris recognition parameter. It is difficult to focus on all of these considerations, but the same category can make the experimental results preliminarily distinguishable.

Because the feature itself is based on the amplitude of the edge detection of the image, certain discriminative differences must exist in the values of the recognition parameters, and the edges overlap. Therefore, the exponential function with e as the base is used to expand the difference such that the iris features can be distinguished. We find a suitable clustering range and range interval through a large number of image training repetitions (in this article, because testers are allowed to repeat shooting, the range interval can be set smaller to improve accuracy in a way that appropriately increases the rejection rate) and clarify the differences in each category the boundaries of the clustering regions such that the feature clustering regions between different categories do not overlap, thereby improving the accuracy of multi-classification. Iris recognition is performed through multiple clustering ranges. With the increase in the number of irises, the accuracy of multi-category recognition of the iris can be effectively improved through continuous adjustment of the feedback learning mechanism.

TABLE 14. Experimental results of add new category recognition experiment.

	The number of correct recognition	The number of false recognition	Correct recognition rate
JLU-4.0	499	1	99.8%
JLU-6.0	500	0	100%
JLU-7.0	500	0	100%

3. Addition of new category recognition experiment

Experimental Setup in This Section: In this section of the experiment, for the case in which the three iris libraries have completed training of 10 categories of recognition models (the number of categories in the multi-class recognition experiment is 10), one category is added (the new category is trained according to the pattern of the single-class recognition experiment). We select 500 images from the original 10 categories for recognition (it has ensured that the accuracy of the 500 images in the original 10 categories is 100%), directly perform experiments in 11 categories (the same testing iris and training iris), observe the change in recognition accuracy, and analyze the impact of the new category on the recognition model. For the multi-source features in the experiment, Gaussian filtering (smoothed) and the equalizing histogram (highlighted) are used as image-processing algorithms.

The recognition of the three iris libraries in 11 categories is shown in TABLE 14.

It can be observed from TABLE 14 that after a new category is added, when the images in the original category are re-recognized, the accuracy does not change substantially, and the accuracy remains high. The result shows that the recognition method in this paper is effective in diluting the differences between different categories. The design of the iris recognition parameters and recognition functions considers

the unpredictability and differences among multi-state irises. It can be observed from the multi-category recognition experiments that the recognition function itself does not calculate the entropy feature values of different categories of the iris images to other iris features. The difference in the small iris value is greatly enlarged when the entropy feature is enlarged, and the category range with the appropriate intervals is used to ensure that the boundaries between different categories do not blend with each other. The effect of this enlargement is:it is remarkable that even after adding new categories, much possibility for adjustment remains, such that high differences occur between different categories, and the recognition boundaries do not interact.

3) STRUCTURAL PROPERTIES AND ALGORITHM INDEPENDENCE

Experimental Setup in This Section: In this section of the experiment, the algorithm independence of the recognition model structure is verified. The algorithm in this paper is replaced with the multi-source image-processing algorithm to verify the relationship between the algorithm structure design and the specific algorithm. Part 1: Feature extraction using only the original image, without feature smoothing and highlighting. Part 2: Replacement of the original Gaussian filtering and equalization histogram with median filtering [30] (smoothed) and the Laplace operator [31] (highlighted). The reason for choosing these two filtering operations is because It is also a common smoothing and highlight filtering image, which has representative. Via these two components of the experiments, the design significance of the multi-source feature fusion of the method in this paper is explained, and the mechanism is independent of the specific algorithm.

In this section of the experiment, the number of iris categories in each of the three iris libraries is set to 10. Each category has 2000 initial training irises. The test iris and training iris of a different category of iris photographed in the same state in each category experiment meet the prerequisites of this paper and exclude extreme interference. The irises to be compared are all irises inside the experimental iris library. In the experiments in this section, the test iris used and the actual number of recognitions are the same (the comparison number for the case in which the number of categories is 10 in TABLE 10-12). The comparison and recognition results of the original image and multi-source fusion in Part 1 of the experiment are shown in TABLE 15. In Part 2 of the experiment, the number of comparisons and recognition of the three iris libraries before and after replacement methods are shown in TABLE 16.

It can be observed from TABLE 15 and TABLE 16 that after the algorithm is changed, the overall recognition effect does not appear to fluctuate greatly, only the original image processing is used, and the recognition effect is greatly reduced. Therefore, it can be concluded that the setting of the multi-source feature fusion mechanism in the method in this paper can improve the recognition effect, but the recognition effect has little correlation with the specific image-processing algorithm. The multi-source processing image mechanism of the method in this paper is designed to achieve the purpose of feature fusion by smoothing processing, highlighting, texture processing and numerical averaging of the original image.

TABLE 15. The number of comparison times and recognition situation.

JLU-4.0 Multi-source fusion		The actual output		Total
		1	0	
The actual category	1	1068	2	1070
	0	0	1489	1489
Total		1068	1491	2559
JLU-4.0 Original		The actual output		Total
		1	0	
The actual category	1	968	102	1070
	0	141	1348	1489
Total		1109	1450	2559
JLU-6.0 Multi-source fusion		The actual output		Total
		1	0	
The actual category	1	3324	4	3328
	0	6	11235	11241
Total		3330	11239	14569
JLU-6.0 Original		The actual output		Total
		1	0	
The actual category	1	2997	331	3328
	0	385	10856	11241
Total		3382	11187	14569
JLU-7.0 Multi-source fusion		The actual output		Total
		1	0	
The actual category	1	2542	2	2544
	0	2	9145	9147
Total		2544	9147	11691
JLU-7.0 Original		The actual output		Total
		1	0	
The actual category	1	2345	199	2544
	0	250	8897	9147
Total		2595	9096	11691

TABLE 16. The number of comparison times and recognition situation.

JLU-4.0 Before replacing methods		The actual output		Total
		1	0	
The actual category	1	1068	2	1070
	0	0	1489	1489
Total		1068	1491	2559
JLU-4.0 After replacing methods		The actual output		Total
		1	0	
The actual category	1	1066	4	1070
	0	1	1488	1489
Total		1067	1492	2559
JLU-6.0 Before replacing methods		The actual output		Total
		1	0	
The actual category	1	3324	4	3328
	0	6	11235	11241
Total		3330	11239	14569
JLU-6.0 After replacing methods		The actual output		Total
		1	0	
The actual category	1	3327	1	3328
	0	3	11238	11241
Total		3330	11239	14569
JLU-7.0 Before replacing methods		The actual output		Total
		1	0	
The actual category	1	2542	2	2544
	0	2	9145	9147
Total		2544	9147	11691
JLU-7.0 After replacing methods		The actual output		Total
		1	0	
The actual category	1	2543	1	2544
	0	3	9144	9147
Total		2546	9145	11691

TABLE 17. The number of iris categories and the number of single-category irises.

Iris use	Category number	Image number in each category	Total
training	30	2000	60000
recognition	30	200	6000

The reason for this design is that in the case of a multi-state iris, it is impossible to determine the appearance status of the iris feature points. Therefore, once the training iris is set in a fixed state, it is easy to increase the difficulty of matching the test iris with the template iris (e.g., the training iris is a defocused image, and the texture is blurred; however, the test iris is a clear image, and the texture is prominent, which causes a large difference between the values after convolution processing). Although training via a large amount of data can make up for this shortcoming, due to the unpredictable state, it is difficult to fully obtain all of the cases when the data set is incomplete, and it is easy to encounter different categories of edge interactions.

Therefore, the method of this paper adopts a neutralization method. By averaging the values of the original image, the smooth image, and the texture highlight image, the values after convolutional processing are concentrated to a certain extent. so as to entropy the subsequent recognition function The clustering of features creates conditions to avoid the adverse effects of highly scattered data on clustering. This mode does not place overly high requirements on the image-processing algorithm itself, and therefore, even if the image-processing algorithm is replaced, the overall recognition effect is not affected.

C. COMPREHENSIVE EXPERIMENT

Experimental Settings: We compare the recognition structure in this paper with multiple recognition methods (localization and normalization adopt this method, the normalized size of the iris recognition area is 180 × 32 dimensions, and the quality confirmation has no effect on iris recognition). The test iris and training iris in the three iris libraries are the same. The number of iris categories and the number of irises in a single category are shown in TABLE 17. The training iris and testing iris meet the prerequisites of this article and exclude extreme cases of interference. For the multi-source features in the experiment, Gaussian filtering (smoothed) and the equalizing histogram (highlighted) are used as image-processing algorithms.

The recognition structure (Case 0) in this paper is compared with the following 20 algorithm combinations:

Traditional Iris Recognition Algorithm:

1. Case 1: Iris recognition with the image processed by the log operator based on Gabor filter optimization and Hamming distance [32] is compared with the traditional Gabor filter and the distance class based on the statistical learning feature extraction parameters.
2. Case 2: The multi-category secondary iris recognition based on the BP neural network after noise reduction by principal component analysis [33] is compared with the recognition method of the traditional BP neural network.
3. Case 3: Iris recognition based on feature weighted fusion [11] and training feature weights through statistical learning is compared with the mode of weighted fusion feature in multiple states.
4. Case 4: A certification function optimization algorithm based on the decision particle swarm optimization algorithm and stable features [10] is compared with the certification model with improved certification function.
5. Case 5: The multi-method parallel decision recognition algorithm for an unsteady iris [12] is compared with the multi-method decision recognition method for an unsteady iris.
6. Case 6: Iris feature representation based on the fractal coding method [34] is compared with the compression fast statistics method for iris texture features in spatial domain feature extraction.
7. Case 7: Iris recognition based on the entropy local binary pattern [35] (ELBP) is compared with the spatial grayscale features in the statistical mode.
8. Case 8: Iris feature extraction and recognition based on image enhancement [36] is compared with the enhanced texture statistical recognition mode under unstable iris features.
9. Case 9: The histogram of oriented gradients (HOG) is used to extract the iris features and authentication by support vector machine (SVM) [37] is compared with the method of manually set labels.
10. Case 10: Ideal iris evidence theory recognition by the clustering method [38] is compared with the recognition model under the clustering feature of the ideal iris set.

Deep Learning Framework Recognition Algorithm:

11. Case 11: Iris recognition and prediction based on multi-view learning classifiers [39] is compared with multi-angle CNN features in statistical learning.
12. Case 12: Iris feature selection and recognition based on the fully and multi-scale convolutional neural network [40] is compared with the cognitive model optimized for convolution kernels.
13. Case 13: Cross-spectral iris recognition based on CNN and supervised discrete hashing [41] is compared with the method of processing data to accommodate the existing recognition functions.
14. Case 14: Concept cognition based on the deep learning neural network [2] is compared with the deep learning architecture cognitive model under a small number of samples.
15. Case 15: A multi-state iris multi-classification recognition method based on statistical cognitive learning [15] is compared with statistically cognitive

methods for a constrained multi-state iris deep learning architecture.

16. Case 16: Iris recognition based on the cognitive internet of things (CIoT) identified by multi-algorithm methods [42] is compared with the cognitive network model combined with big data analysis.
17. Case 17: The iris recognition method based on the iris-specific Mask R-CNN [9] is compared with iris recognition in the deep learning architecture mode.
18. Case 18: An iris recognition method based on error correction codes and convolutional neural networks [17] is compared with error correction codes in the label classification mode.
19. Case 19: The statistical learning model of convolutional neural networks based on the VGG16 model architecture [43] is compared with the recognition effect under the classic CNN architecture.
20. Case 20: The Faster R-CNN Inception Resnet V2 model architecture [44] for iris recognition is compared with the recognition effect under other classic CNN architectures.

The recognition results of all 21 cases in the three libraries are shown in TABLE 18.

From the experimental results in TABLE 18, it can be observed that the experimental results of the three iris banks are relatively consistent, and the recognition model structure in this paper has the highest recognition rate for detection of constrained multi-state irises. The experimental results of each method are analyzed in TABLE 18:

In Case 1, the log operator eliminates the image noise and highlights the iris texture. By analyzing the experimental results, it can be found that the Hamming distance is suitable for distinguishing irises with large differences in different categories of the same collected state. The thresholds used in distinguishing cannot be satisfactorily set for multi-state irises with differences in the same category. In addition, optimization of the Gabor filter depends on the recognition effect of the training iris. Therefore, in the case of the test irises collected in different states of the training iris, the method has a low correct recognition rate.

In Case 2, the secondary recognition method takes Gabor + Hamming distance recognition as the first recognition, and the second recognition is conducted by the Haar + BP neural network. The dimension of the iris data is compressed by principal component analysis (PCA) [45]. This approach is better than the pure Hamming distance, and multi-classification is converted into single classification. However, due to the complex structure of the BP neural network and the large adjustment parameters, adjustment of the multi-state iris might cause over-fitting, leading to low recognition accuracy of the multi-state iris.

In Case 3, the features are extracted by the Haar wavelet and LBP method. Via the result of a certain number of training irises, the recognition weights of the two methods are

TABLE 18. The recognition results of all 21 cases in three libraries.

JLU-4.0		
Case	The number of correctly recognition	CRR
0	**5998**	**99.9667%**
1	4498	74.9667%
2	5218	86.9667%
3	4980	83.0000%
4	5369	89.4833%
5	5789	96.4833%
6	5568	92.8000%
7	5087	84.7833%
8	4687	78.1167%
9	4031	67.1833%
10	5846	97.4333%
11	4698	78.3000%
12	5213	86.8833%
13	5512	91.8667%
14	4497	74.9500%
15	5974	99.5667%
16	5847	97.4500%
17	5231	87.1833%
18	5120	85.3333%
19	4985	83.0833%
20	5436	90.6000%
JLU-6.0		
Case	The number of correctly recognition	CRR
0	**6000**	**100%**
1	4523	75.3833%
2	4956	82.6000%
3	4723	78.7167%
4	5489	91.4833%
5	5789	96.4833%
6	5359	89.3167%
7	5152	85.8667%
8	4412	73.5333%
9	4756	79.2667%
10	5842	97.3667%
11	4863	81.0500%
12	5012	83.5333%
13	5612	93.5333%
14	4423	73.7167%
15	5955	99.2500%
16	5710	95.1667%
17	5321	88.6833%
18	5120	85.3333%
19	5036	83.9333%
20	4987	83.1167%
JLU-7.0		
Case	The number of correctly recognition	CRR
0	**5999**	**99.9833%**
1	4465	74.4167%
2	5023	83.7167%
3	4698	78.3000%
4	5314	88.5667%
5	5568	92.8000%
6	5169	86.1500%
7	4823	80.3833%
8	4423	73.7167%
9	4752	79.2000%
10	5785	96.4167%
11	5023	83.7167%
12	5203	86.7167%
13	5553	92.5500%
14	4512	75.2000%
15	5978	99.6333%
16	5862	97.7000%
17	5217	86.9500%
18	5324	88.7333%
19	4975	82.9167%
20	5198	86.6333%

calculated. According to the recognition weights, the final conclusion is obtained. In the case in which other conditions are ideally set, the proposed method has a comparative advantage if there is only one diversification factor. However, the weight judgment method based on feedback of the recognition result cannot accurately determine the influence degree of multiple diversification factors on iris recognition. Therefore, the combination of multiple diversification factors has poor recognition effects.

In Case 4, the decision particle swarm optimization algorithm and the stability feature algorithm are designed by modifying the recognition function, which can improve the environmental inclusiveness of the model and the accuracy. However, this algorithm requires a large amount of iris data for training. In the case in which the iris dataset cannot meet the actual training requirements, the recognition accuracy is not as good as that of the algorithm in this paper.

In Case 5, the multi-method parallel decision recognition algorithm for a multi-state iris is a multi-method decision mode for a multi-state iris. First, the iris image is processed via multiple image-processing methods, and stable iris features are extracted and recognized by a multi-algorithm. According to a large number of training iris recognition repetitions in different environments, we judge the credibility of the method in different environments and choose the most credible method for recognition. The environmental tolerance of this method and the recognition of unsteady-state iris features have notably good improvements, and thus, the accuracy is high. However, the reliability of this method depends on the performance of the recognition algorithm itself (the examples in this article are mainly Gabor + Hamming and Haar + BP neural networks), and certain requirements exist for the iris dataset (a large amount of training data). The correct recognition rate is not as good as that of the method proposed in this paper.

In Case 6, the iris feature representation method based on the fractal coding method is suitable for the iris image. The iris is block compressed and encoded by enhancing the differences. This method can conserve coding space and improve efficiency, but it might reduce the range of recognizable irises and the effective amount of information in the iris, leading to more errors in recognition.

In Case 7, iris recognition based on the entropy local binary pattern describes the entropy information as the local binary pattern histogram in one-dimensional space for iris feature extraction. The recognition effect of the method is improved to a certain extent. However, the training set belongs to the non-ideal training set. ELBP is designed for the iris set with stable and small differences in an ideal state. Therefore, ELBP can obtain good results in the ideal state iris set experiment, whereas the non-ideal state iris set has poor performance.

In Case 8, iris feature extraction based on image enhancement can be conducted to highlight the iris texture by image edge detection. This method can be used to suppress the interference of noise and redundancy. The diversification factors of the multi-state iris are somewhat inclusive. However, compared with the proposed method, the range of available irises is still smaller. Therefore, the recognition accuracy is relatively poor.

In Case 9, the recognition method based on the histogram of oriented gradients (HOG) and SVM recognizes the change rule between the gray values of each point of the iris as a feature. For a large number of training images, the process of making labels by hand is too cumbersome and subjective and easily leads to cognitive bias. For multi-state irises (such as blurred images, etc.), it is difficult for HOG to accurately reflect the iris grayscale changes among the points, and thus, the overall recognition rate is quite poor.

In Case 10, the recognition method of iris evidence theory based on the clustering method finds common points of the training iris data according to the clustering method and determines the iris features. For an ideal iris, such algorithms can better reflect the convergence of the iris. The selection of cluster-like points and non-ideal image iris cluster points are relatively complicated, resulting in a reduction in recognition rate.

In Case 11, the recognition method based on multi-view learning classifier recognition prediction adjusts the convolutional layer to extract multi-angle iris features for statistical analysis, but the experimental iris set of this method is an ideal iris, and thus, the iris clustering effect is better. For multi-state irises such as blurred images, the setting of the convolutional layer should be more accurate such that the iris features of different states can be effectively concentrated together. The recognition accuracy of this method is not as good as the method of this paper.

In Case 12, feature selection and recognition in the convolutional neural network based on FMnet is also optimized for convolution kernels such that the system can better apply cognitive learning and improve the correct recognition rate of the iris under different resolutions. Although this method improves the incomplete shortcomings of manual label setting, iris feature extraction for feature vectors implies certain requirements on image quality, which is not conducive to cognitive learning of the multi-state iris.

In Case 13, cross-spectral iris recognition using CNN and supervised discrete hashing is a supervised discrete hash operation of the self-learning features of conventional CNN convolution-processed images by cross-spectral methods, and segmentation recognition is performed by Softmax [46] cross entropy loss. This type of method is applied to the iris data to better adapt to the existing recognition function, thereby improving the iris recognition accuracy. However, the classification effect of the existing Softmax function is limited, which might cause interference in the data processing of the multi-state iris and is not conducive to multi-category recognition.

In Case 14, the concept recognition algorithm based on the deep learning neural network is currently the most common recognition method, but because a single deep learning architecture method contains requirements for data volume and

data classification, data state classification and data volume cannot be completely performed in an unsteady iris. In the case of complete deficiency, the advantages of deep learning are difficult to access, which also leads to a low recognition rate of the single deep learning architecture.

In Case 15, the convolutional neural network recognition method based on constrained multi-state iris statistical cognitive learning is a design similar to the environment used in this paper. This method recognizes labels through a certain number of irises and increases the number of different categories through the dilution layer. The degree of discrimination has a good recognition accuracy. At the same time, many images in the unrecognizable iris can also be identified by this method. The accuracy rate is not as good as that of the method proposed in this paper because in non-linear expansion of the recognition function, the method of Case 15 designs a dilution layer separately for the decimal component of the recognition result of the fully connected layer and sets the dilution step to expand the discrimination. Compared with the method in this paper, the optimization parameter structure is more complicated and more constrained. Therefore, compared with the method of direct expansion of feature parameters in this paper, the expansion effect is worse, and the degree of discrimination has a certain coincidence, and therefore, the recognition rate in this paper is higher.

In Case 16, the CIoT method constructed by the multi-algorithm method is similar to the proposed method, both of which belong to statistical cognitive learning methods. The cognitive internet is used in iris recognition in CIoT. For different features, iris concept statistical cognition is performed using the multi-algorithm method to ensure the accuracy of iris feature recognition. However, the method requires a higher effective information quantity than the proposed method, and the iris processing process should be more precise, making the recognition accuracy lower than that of the proposed method.

In Case 17, the iris recognition method based on the iris-specific mask R-CNN is a method for the overall flow of the iris, which is improved based on the existing iris recognition architecture to improve the iris recognition rate. The existing architecture is affected by the architecture design, and certain constraints exist. The low recognition rate of this method occurs because in the prerequisites of this paper, the number of irises is not large, and it is difficult to guarantee the training of iris features in various situations, thus reducing the accuracy.

In Case 18, the iris recognition method based on the error correction code and the convolutional neural network uses the error correction code to classify the texture state of the iris during training, thereby effectively improving the recognition of the iris with high flexibility. However, because the amount of iris data is insufficient, cognition of the iris is limited overall, and the existing CNN architecture does not necessarily apply to all unsteady-state iris images without improvements.

In Case 19, the VGG16 model is composed of 13 convolutional layers and 3 fully connected layers. In iris recognition, the iris image is continuously convolved, pooled, and ReLU processed to obtain different types of feature values, thereby performing iris certification. However, due to the prerequisites in this paper, the iris initial training data are not classified in detail and are lightweight, and the number of samples is far from the standard for deep learning. Therefore, it is difficult to take advantage of the superiority of the VGG16 model. These factors greatly reduce the recognition accuracy of the VGG16 model.

In Case 20, the Faster R-CNN Inception Resnet V2 model architecture is a more advanced convolutional neural network model that allows training on lightweight data compared with the VGG16 model, thus reducing the difficulty of training. However, under the prerequisites of the unsteady-state iris targeted in this paper, although the architecture model reduces the training complexity, too many redundant features are counted during training, which creates interference. Considering the changes in the iris acquisition status and the use conditions of the existing architecture, the model does not have a high degree of matching for the untrained components, making its sensitivity to the unsteady iris unpredictable and low, which can reduce the recognition accuracy of the model.

In summary, the recognition model in this paper considers the connection between feature expression and recognition, avoids the shortcomings of low adaptability between the two components caused by segmentation of the entire process machinery, and solves the correlation between the feature expression and the recognition problem. Knowledge cognition is the main factor, and the concept of each component is established to prevent the problem of insufficient learning that restricts the different states of the multi-state iris due to the fixed threshold. Aimed at the lack of data sets and data classification, the characteristics of the iris are expressed through multiple sources, and the existing single deep learning architecture model is improved. A new recognition function was designed to improve the degree of discrimination between different categories, thereby improving the recognition accuracy of multi-category classification of the lightweight category of the recognition model and the capability of heterogeneous iris recognition.

IV. CONCLUSION

Aimed at the constrained multi-state iris caused by different devices and environments, this paper proposes a heterogeneous iris recognition method based on the entropy feature lightweight neural network. Under the premise of ensuring that the processing does not affect feature expression and recognition, the traditional processing method of a single-source iris in a non-steady-state iris is mostly ineffective, and the existing iris data set size and situation classification constraints make it difficult to address single questions related to the requirements of the learning methods in the framework of deep learning. The method of this paper is oriented to conceptual cognition and design of a series of closely related links. The results of different iris libraries demonstrate that the design of each component of the method is reasonable and

meaningful. The accuracy of multi-category classification in different iris libraries is maintained at a high level, the recognition range is wide, and with use of the dynamic learning mechanism of feedback, experts can dynamically adjust the model according to the results.

This paper focuses on identifying the forward process. For the reverse optimization portion, only the relevant mechanism is designed. Future research will focus on how to more fully automate the mechanism, allow the system perform unsupervised learning, and design the overall identification process.

ACKNOWLEDGMENT

The authors would like to thank the referee's advice.

REFERENCES

[1] F. Alonso-Fernandez, R. A. Farrugia, J. Bigun, J. Fierrez, and E. Gonzalez-Sosa, "A survey of super-resolution in iris biometrics with evaluation of dictionary-learning," *IEEE Access*, vol. 7, pp. 6519–6544, 2019.

[2] T. Zhao, Y. Liu, G. Huo, and X. Zhu, "A deep learning iris recognition method based on capsule network architecture," *IEEE Access*, vol. 7, pp. 49691–49701, 2019.

[3] (2018). *CASIA Iris Database*. [Online]. Available: http://www.cbsr.ia.ac.cn/china/Iris%20Databases%20CH.asp

[4] (2019). *Ubiris Database*. [Online]. Available: http://iris.di.ubi.pt/ubiris2.html

[5] Y. Lee, K. Kim, T. Hoang, M. Arsalan, and K. Park, "Deep residual CNN-based ocular recognition based on rough pupil detection in the images by NIR camera sensor," *Sensors*, vol. 19, no. 4, p. 842, Apr. 2019.

[6] S. Bazrafkan, S. Thavalengal, and P. Corcoran, "An end to end deep neural network for iris segmentation in unconstrained scenarios," *Neural Netw.*, vol. 106, pp. 79–95, Oct. 2018.

[7] M. S. V. Kumar, and R. Gunasundari, "Computer-aided diagnosis of anterior segment eye abnormalities using visible wavelength image analysis based machine learning," *J. Med. Syst.*, vol. 42, no. 7, p. 128, Jul. 2018.

[8] Q. Yu, H. Tang, K. C. Tan, and H. Yu, "A brain-inspired spiking neural network model with temporal encoding and learning," *Neurocomputing*, vol. 138, pp. 3–13, Aug. 2014.

[9] Z. Zhao and A. Kumar, "A deep learning based unified framework to detect, segment and recognize irises using spatially corresponding features," *Pattern Recognit.*, vol. 93, pp. 546–557, Sep. 2019.

[10] L. Yuanning, L. Shuai, and Z. Xiaodong, "Iris secondary recognition based on decision particle swarm optimization and stable texture," *J. Jilin Univ. (Eng. Technol. Ed.)*, vol. 49, no. 4, pp. 1329–1338, Jul. 2019.

[11] L. Yuanning, L. Shuai, and Z. Xiaodong, "Iris recognition algorithm based on feature weighted fusion," *J. Jilin Univ. (Eng. Technol. Ed.)*, vol. 49, no. 1, pp. 221–229, Jan. 2019.

[12] L. Shuai, L. Yuanning, Z. Xiaodong, Z. Kuo, D. Tong, L. Xinlong, and W. Chaoqun, "Unsteady state lightweight iris certification based on multi-algorithm parallel integration," *Algorithms*, vol. 12, no. 9, p. 194, 2019.

[13] W. Bouamra, C. Djeddi, B. Nini, M. Diaz, and I. Siddiqi, "Towards the design of an offline signature verifier based on a small number of genuine samples for training," *Expert Syst. Appl.*, vol. 107, pp. 182–195, Oct. 2018.

[14] M. Arsalan, D. S. Kim, M. B. Lee, M. Owais, and K. R. Park, "FRED-net: Fully residual encoder–decoder network for accurate iris segmentation," *Expert Syst. Appl.*, vol. 122, pp. 217–241, May 2019.

[15] L. Shuai, L. Yuanning, Z. Xiaodong, H. Guang, C. Jingwei, Z. Qixian, W. Zukang, and D. Zhiyi, "Statistical cognitive learning and security output protocol for multi-state iris recognition," *IEEE Access*, vol. 7, pp. 132871–132893, Sep. 2019.

[16] Z. Wang, C. Li, H. Shao, and J. Sun, "Eye recognition with mixed convolutional and residual network (MiCoRe-net)," *IEEE Access*, vol. 6, pp. 17905–17912, Mar. 2018.

[17] Y. Cheng, Y. Liu, X. Zhu, and S. Li, "A multiclassification method for iris data based on the Hadamard error correction output code and a convolutional network," *IEEE Access*, vol. 7, pp. 145235–145245, Oct. 2019.

[18] L. Shuai, Y. Liu, X. Zhu, G. Huo, J. Cui, Q. Zhang, Z. Dong, and X. Jiang, "Current optimal active feedback and stealing response mechanism for low-end device constrained defocused iris certification," *J. Electron. Imag.*, vol. 29, no. 1, Jan. 2020, Art. no. 013012.

[19] N. Liu, J. Liu, Z. Sun, and T. Tan, "A code-level approach to heterogeneous iris recognition," *IEEE Trans. Inf. Forensics Secur.*, vol. 12, no. 10, pp. 2373–2386, Oct. 2017.

[20] E. G. Llano, M. S. García Vázquez, J. M. C. Vargas, L. M. Z. Fuentes, and A. A. Ramírez Acosta, "Optimized robust multi-sensor scheme for simultaneous video and image iris recognition," *Pattern Recognit. Lett.*, vol. 101, pp. 44–51, Jan. 2018.

[21] B. Subramani and M. Veluchamy, "Fuzzy contextual inference system for medical image enhancement," *Measurement*, vol. 148, Dec. 2019, Art. no. 106967.

[22] Y. Zhang, S. Li, and X. Liu, "Neural network-based model-free adaptive near-optimal tracking control for a class of nonlinear systems," *IEEE Trans. Neural Netw. Learn. Syst.*, vol. 29, no. 12, pp. 6227–6241, Dec. 2018.

[23] H. Shi, Y. Zhang, Z. Zhang, N. Ma, X. Zhao, Y. Gao, and J. Sun, "Hypergraph-induced convolutional networks for visual classification," *IEEE Trans. Neural Netw. Learn. Syst.*, vol. 30, no. 10, pp. 2963–2972, Oct. 2019.

[24] L. Shuai, L. Yuanning, and Z. Xiaodong, "Constrained sequence iris quality evaluation based on causal relationship decision reasoning," presented at the 14th Chin. Conf. Biometric Recognit. (CCBR), Zhuzhou, China, Oct. 2019.

[25] P. Kunakornvong and P. Sooraksa, "Unified histogram equalization for defect detection on air bearing surfaces," *Int. J. Innov. Comput. Inf. Control*, vol. 13, no. 1, pp. 1–21, Feb. 2017.

[26] L. Shuai, L. Yuanning, and Z. Xiaodong, "Iris location algorithm based on partitioning search," *Comput. Eng. Appl.*, vol. 54, no. 18, pp. 212–217, Sep. 2018.

[27] (2018). *JLU Iris Image Database*. [Online]. Available: http://www.jlucomputer.com/index/irislibrary/irislibrary.html

[28] W. Yang, X. Zhang, and J. Li, "A local multiple patterns feature descriptor for face recognition," *Neurocomputing*, vol. 373, pp. 109–122, Jan. 2020.

[29] D. Krenn, V. Suppakitpaisarn, and S. Wagner, "On the minimal Hamming weight of a multi-base representation," *J. Number Theory*, vol. 208, pp. 168–179, Mar. 2020.

[30] D. Cheng and K. I. Kou, "Multichannel interpolation of nonuniform samples with application to image recovery," *J. Comput. Appl. Math.*, vol. 367, Mar. 2020, Art. no. 112502.

[31] S. Biagi and T. Isernia, "On the solvability of singular boundary value problems on the real line in the critical growth case," *Discrete Continuous Dyn. Syst. A*, vol. 40, no. 2, pp. 1131–1157, 2020.

[32] Y.-N. Liu, S. Liu, X.-D. Zhu, Y.-H. Chen, S.-G. Zheng, and C.-Z. Shen, "LOG operator and adaptive optimization Gabor filtering for iris recognition," *J. Jilin Univ. (Eng. Technol. Ed.)*, vol. 48, no. 5, pp. 1606–1613, Sep. 2018.

[33] S. Liu, Y. Liu, X. Zhu, Z. Lin, and J. Yang, "Ant colony mutation particle swarm optimization for secondary iris recognition," *J. Comput.-Aided Des. Comput. Graph.*, vol. 30, no. 9, pp. 1604–1614, 2018.

[34] N. M. G. Al-Saidi, A. J. Mohammed, R. J. Al-Azawi, and A. H. Ali, "Iris Features Via Fractal Functions for Authentication Protocols," *Int. J. Innov. Comput. Inf. Control*, vol. 14, no. 4, pp. 1441–1453, Aug. 2019.

[35] B. Sree Vidya and E. Chandra, "Entropy based local binary pattern (ELBP) feature extraction technique of multimodal biometrics as defence mechanism for cloud storage," *Alexandria Eng. J.*, vol. 58, no. 1, pp. 103–114, Mar. 2019.

[36] M. Zhang, Z. He, H. Zhang, T. Tan, and Z. Sun, "Toward practical remote iris recognition: A boosting based framework," *Neurocomputing*, vol. 330, pp. 238–252, Feb. 2019.

[37] C. M. Patil and S. Gowda, "An approach for secure identification and authentication for biometrics using iris," presented at the Int. Conf. Current Trends Comput., Elect., Electron. Commun. (CTCEEC), Mysore, India, Sep. 2017.

[38] T. Ma and F. Xiao, "An improved method to transform triangular fuzzy number into basic belief assignment in evidence theory," *IEEE Access*, vol. 7, pp. 25308–25322, 2019.

[39] A. Kuehlkamp, A. Pinto, A. Rocha, K. W. Bowyer, and A. Czajka, "Ensemble of multi-view learning classifiers for cross-domain iris presentation attack detection," *IEEE Trans. Inf. Forensics Secur.*, vol. 14, no. 6, pp. 1419–1431, Jun. 2019.

[40] R. Tobji, W. Di, and N. Ayoub, "FMnet: Iris segmentation and recognition by using fully and multi-scale CNN for biometric security," *Appl. Sci.*, vol. 9, no. 10, p. 2042, May 2019.
[41] K. Wang and A. Kumar, "Cross-spectral iris recognition using CNN and supervised discrete hashing," *Pattern Recognit.*, vol. 86, pp. 85–98, Feb. 2019.
[42] R. Gad, M. Talha, A. A. A. El-Latif, M. Zorkany, A. El-Sayed, N. El-Fishawy, and G. Muhammad, "Iris recognition using multi-algorithmic approaches for cognitive Internet of Things (CIoT) framework," *Future Gener. Comput. Syst.*, vol. 89, pp. 178–191, Dec. 2018.
[43] Á. Arcos-García, J. A. Álvarez-García, and L. M. Soria-Morillo, "Evaluation of deep neural networks for traffic sign detection systems," *Neurocomputing*, vol. 316, pp. 332–344, Nov. 2018.
[44] F. Gao, T. Huang, J. Wang, J. Sun, A. Hussain, and E. Yang, "Dual-branch deep convolution neural network for polarimetric SAR image classification," *Appl. Sci.*, vol. 7, no. 5, p. 447, 2017.
[45] L. Huang, Y. Yang, X. Zhao, C. Ma, and H. Gao, "Sparse data-based urban road travel speed prediction using probabilistic principal component analysis," *IEEE Access*, vol. 6, pp. 44022–44035, Aug. 2018.
[46] P. Tschandl, G. Argenziano, M. Razmara, and J. Yap, "Diagnostic accuracy of content-based dermatoscopic image retrieval with deep classification features," *Brit. J. Dermatol.*, vol. 181, no. 1, pp. 155–165, Jul. 2019.

LIU SHUAI received the M.S. degree from Jilin University, China, in 2019, where he is currently pursuing the Ph.D. degree. His research interests include applications of computer vision and iris recognition.

LIU YUANNING received the Ph.D. degree from Jilin University, China, in 2004. He completed the Ph.D. research with the University of Vienna, Austria, in 2007. He was a Visiting Scholar with the University of Missouri, USA, in 2015. He is currently a Professor of computer science with Jilin University. His research interests include software engineering, iris biometrics, pattern recognition, and bioinformatics.

ZHU XIAODONG received the Ph.D. degree from Jilin University, China, in 2004. He is currently a Professor of computer science with Jilin University. His research interests include software engineering, pattern recognition, and machine learning techniques for biometrics.

HUO GUANG received the Ph.D. degree from Jilin University, China, in 2016. He is currently an Associate Professor with Northeast Electric Power University. His research interests include pattern recognition, machine learning, biometrics, and image processing.

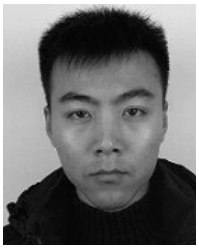

CUI JINGWEI is currently pursuing the master's degree with Jilin University, China. His research interests include applications of computer vision and iris recognition.

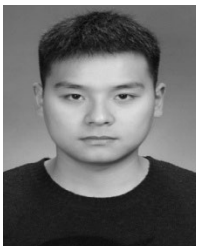

ZHANG QIXIAN is currently pursuing the master's degree with Jilin University, China. His research interests include applications of computer vision and iris recognition.

WU ZUKANG is currently pursuing the master's degree with Jilin University, China. His research interest includes iris recognition.

LI XINLONG is currently pursuing the master's degree with Jilin University, China. His research interest includes iris recognition.

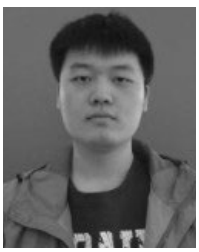

WANG CHAOQUN is currently pursuing the master's degree with Jilin University, China. His research interest includes iris recognition.